Analysis of Chinese Hamster Ovary cells during batch culture using flow cytometry

Diplomarbeit

zur Erlangung des akademischen Grades
Diplomingenieur

durchgeführt am **Institut für Angewandte Mikrobiologie (IAM)**

eingereicht am 20.10.2008

von **MANUEL MATEJ**

Betreuer: Nicole Borth, Ao.Univ.Prof. Dipl.-Ing. Dr.nat.techn

Matrikelnummer 9940403

Foreword

I want to thank everybody who invested their time and patience on me during studying.

- Special thanks to my supervisor Ao. Univ. Prof. Dipl.-Ing Dr. nat. techn. Nicole Borth for her intense and inspiring assistance. Her comprehensive knowledge about Flow cytometry made it possible for me to complete this work successfully.

- Many thanks to the cell culture group at the Institute for Applied Microbiology, specially Georg Hinterkörner, who was willing to back me at all time.

- At last but not least I want to thank my family and friends, who accompanied me through my time of study.

Danksagung

Für ihren Beitrag zum Gelingen dieser Arbeit möchte ich mich besonders bei folgenden Menschen bedanken:

- Ao. Univ. Prof. Dipl.-Ing Dr. nat. techn. Nicole Borth meiner unmittelbaren Betreuerin für ihre ausgezeichnete Einführung in das Denken und Arbeiten in der tierischen Zellkultur. Durch ihr umfangreiches Fachwissen speziell die Durchflusszytometrie (FACS) betreffend, wurde mir die erfolgreiche Durchführung dieser Arbeit möglich gemacht.

- Der Gruppe für tierische Zellkultur des Instituts für Angewandte Mikrobiologie, speziell an Georg Hinterkörner, der mir immer hilfreich zur Seite stand.

- Meinen Freunden und Freundinnen, die mich während des Studiums in welcher Form auch immer begleitet haben.

- Bei meiner Mutter**,** die mir stets ein Zuhause bietet, in dem ich mich gerne entspanne und das mir Kraft gibt. Des weiteren für ihre finanzielle Unterstützung und ihr uneingeschränktes Vertrauen in mich und meine Fähigkeiten während meines gesamten Studiums.

Contents

1. Zusammenfassung

Das Ziel dieser Arbeit war es Korrelationen zwischen dem Zustand der Zelle, deren Physiologie und verschiedenen Fluoreszenzfärbeprotokollen zur Überwachung und Auswahl zu identifizieren. Um dies zu erreichen analysierten wir verschiedene Batchkulturen von Ovarienzelllinien chinesischer Hamster. Zur Charakterisierung des zellulären Zustandes während der Batchkultur wurden Substrataufnahme, Laktatproduktion, die Anzahl viabler Zellen und die Viabilität festgestellt. Gleichzeitig wurde mittels Flow Cytometry der Gehalt an Glutathion, reaktiver Sauerstoffspezies und zellulärer Autofluoreszenz bestimmt.

Die gewonnen Daten zeigten eindeutig große Unterschiede zwischen Wirtszelllinien und Produktionszelllinien. In Wirtszellen korrelierte zu Beginn der Anteil an reaktiver Sauerstoffspezies mit der metabolischen Rate. Nachdem das Substrat erschöpft ist, steigt der Anteil an reaktiver Sauerstoffspezies an, da die zelluläre Abwehr nicht mehr ausreicht. Unter den beobachteten Produktionszelllinien konnten keine derartigen Korrelationen festgestellt werden. In Wirts- und in Produktionszelllinien verringerten sich die zellulären Glutathionlevel bei geringerer Substratverfügung.

2. Abstract

Aim of the study was to identify correlations between cellular state, physiology and different fluorescent staining protocols for monitoring and screening. To achieve this we analysed batch cultures of several Chinese Hamster Ovary (CHO) cell lines. Substrate uptake, lactate production, viable cell count and viability were measured to characterise the cellular state during the batch processes. Simultaneously the content of glutathione (GSH), Reactive Oxygen Species (ROS), as well as cellular autofluorescence were determined by flow cytometry.

The obtained data shows that there are in fact major differences between host cell lines and production cell lines. In host cells content of ROS initially correlates to the metabolic rate. After substrate is depleted, intracellular ROS rises, as the cellular defense fails. Among the observed production cells no such correlations could be measured. In both host and production cells, cellular glutathione levels are decreasing with decreasing substrate availability.

3. Abbreviations

FACS Fluorescent Activated Cell Sorting

MCB Monochlorobimane

CHO Chinese Hamster Ovary Cells

DCF Carboxy-2', 7'-dichlorofluorescein

DCFH 2′7′-dichlorofluorescin

$DCFH_2$ 2',7'-Dichlorodihydrofluorescein

ROS Reactive Oxygen Species

GSH Glutathione

4. Introduction

4.1 Important parameters for monitoring cellular state and physiology

4.1.1 Glucose

Cellular respiration consists of several metabolic reactions and processes that take place in organisms' cells to convert biochemical energy from nutrients as glucose into adenosine triphosphate. Glucose is taken up by the cells directly out of the culture medium.

4.1.2 Glutamine

Glutamine is an amino acid and belongs to the nutrients needed for the cellular respiration. Like glucose it is supplemented to the culture medium and taken up by the cells.

4.1.3 Lactate

Lactate is a product of the glucolytic pathway. Instead of degradation via the citric acid cycle, glucose is converted to lactate and NAD+.

4.1.4 Glutathione

GSH is a tripeptide of cysteine, glycine, and glutamic acid. It is considered as the most important part of the cellular defense system against ROS and ranked among antioxidants [1]. This is underlined by the fact that the cell invests 10 to 20 % of its energy into the generation of GSH. All thiol groups are kept in a reduced state at a concentration of approximately 5 mM in animal cells. GSH reduces any disulfide bonds formed within cytoplasmic proteins to cysteines by acting as an electron donor.

Under normal conditions GSH is found exclusively in its reduced form, because the enzyme that oxidises it, the glutathione reductase, is constitutively active and can be induced upon oxidative stress. The ratio of reduced GSH to oxidized GSH within cells is used scientifically to measure cellular toxicity and oxidative stress.

GSH is not an essential nutrient since it can be synthesized from the amino acids L-cysteine, L-glutamate and glycine.

4.1.4.1 Synthesis of glutathione

1. Synthesis of gamma-glutamylcysteine from L-glutamate and cysteine via the enzyme gamma-glutamylcysteine synthetase. This reaction is the limiting step in the GSH synthesis.
2. Linkage of glycine to the C-terminal of gamma-glutamylcysteine via the enzyme glutathione synthetase.

All cells in the human body are capable of synthesising GSH, but liver GSH synthesis seems to be essential.

4.1.4.2 Function of glutathione

<u>General</u>

The thiol group of cysteine in reduced GSH, is able to donate a reducing equivalent ($H^+ + e^-$) to unstable molecules, such as ROS. In despensing one electron, GSH itself becomes reactive, but ready to react with another reactive GSH to form glutathione disulfide. This reaction is only possible because the concentration of GSH in cells is very high (up to 5 mM in the liver). GSH is regenerated from glutathione disulfide by the enzyme glutathione reductase.

In healthy cells and tissue, more than 90% of the total GSH pool is found to be in its reduced state and usually less than 10% is existing in the disulfide form.

In the cell GSH is an important substrate in conjugation reactions and reduction reactions, which are catalysed by the glutathione S-transferase enzymes in cytosol, microsomes, and mitochondria.

GSH participates in synthesis of leukotriene and is important as a hydrophilic molecule that is added to lipophilic toxins and waste in the liver during biotransformation before they can become part of the bile. GSH is needed for the detoxification of methylglyoxal, which is a toxin produced as a by-product of metabolism.

Resistance to cytotoxic and immunotoxic effects of mercury

MCB was used to find out the positve effects of GSH regarding intacelluar resistance to cytotoxic an immunotoxic effects of mercury in lymphocytes and monocytes [2]. T and B-cells were stained with MCB and separated into high and low fluorescent groups by FACS analysis. Shenker BJ. (1993) found that cells with high GSH fluorescence were resistant to the cytotoxic and immunotoxic effects of mercury.

In contrast, cells with low levels of GSH were extremely sensitive to mercury.
All cells exhibited a dose-dependent decrease in GSH content coupled with a reduction in GSH/glutathione disulfide levels.

GSH levels were also reduced in monocytes following exposure to mercury. Glutathione disulfide levels levels remained constant and a decline in the GSH/glutathione disulfide levels ratio was observed.

For all cell types, mercury did not inhibit the activities of GSH reductase and GSH peroxidase, enzymes responsible for oxidation/reduction of GSH and glutathione disulfide.

It was concluded that susceptibility to the immunotoxic effects of mercury is, in part, dependent upon GSH levels and further that mercury inhibits GSH generation in lymphocytes and monocytes.

Glutathione and its association with overexpression of bcl-xL.

Cells are known to die by different pathways including apoptosis, or programmed cell death, and necrosis [3]. The bcl-xL gene is a member of a family of genes regulating apoptosis, and often inhibits death like the prototype of this family, bcl-2. Xu L et al. (1999) studied ischemia-like injury by overexpressing the anti-cell death gene bcl-xL.

Bcl-xL is important for normal brain development. Then antioxidant effects were assessed by measuring GSH using MCB. As a result protection by bcl-xL was found against glucose deprivation and hydrogen peroxide exposure, but not combined oxygen and glucose deprivation.

Overexpression of bcl-xL was associated with elevated glutathione levels. The increased glutathione contributed to the protection from glucose deprivation. It was concluded that the increased antioxidant defense observed should be beneficial against apoptotic and necrotic cell death.

4.1.5 Reactive Oxygen Species

ROS are compounds which occur in the cell when it suffers from any kind of negativ influences.

4.1.5.1 Formation of Reactive Oxygen Species

ROS, comprising superoxide anion ($O_2^{\bullet -}$), hydroxyl radicals ($OH^{\bullet}$), and hydrogen peroxide (H_2O_2), are generated during aerobic metabolism [4].

The mitochondrion is the most important source of ROS production. Other cellular sources are, enzymes, such as cytochrome P450 in the endoplasmic reticulum (ER), lipoxygenases, cyclooxygenases, Xanthine oxidase, and the NADPH oxidase of white blood cells. Under normal physiological conditions,

about 1–3 % of electrons carried by the mitochondrial electron transport chain divert from the pathway and pass directly to oxygen, generating $O_2^{\bullet -}$ [1].

The Mitochondrial respiratory complex I, also known as the NADH-ubiquinone oxidoreductase, is an important source of ROS production [4]. Respiratory complex III, also known as the ubiquinol-cytochrome c oxidoreductase, as well as the coenzyme Q radical generated during the Q cycle, is believed to be the site with the highest quantity of mitochondrial $O_2^{\bullet -}$ production [1]. The enzyme manganese superoxide dismutase in the mitochondrial matrix ensures that the level of $O_2^{\bullet -}$ formed during normal electron transport is kept at a level which does not damage proteins of the matrix involved in the regulation of metabolism. Such proteins are the iron sulfur proteins aconitase and succinate dehydrogenase [5].

Manganese superoxide dismutase catalyzes the breakdown of $O_2^{\bullet -}$ to yield H_2O_2, which is an important signaling molecule generated throughout the animal kingdom. Under normal circumstances, H_2O_2 generated by the dismutation of mitochondrial $O_2^{\bullet -}$ is broken down by a glutathione-dependent peroxidase enzyme to yield water, whereas in the cytosol H_2O_2, which is generated by peroxisomal b-oxidation of fatty acids or by the enzyme Xanthine oxidase, it is broken down by catalase and glutathione-dependent peroxidase enzyme (see figure 1).

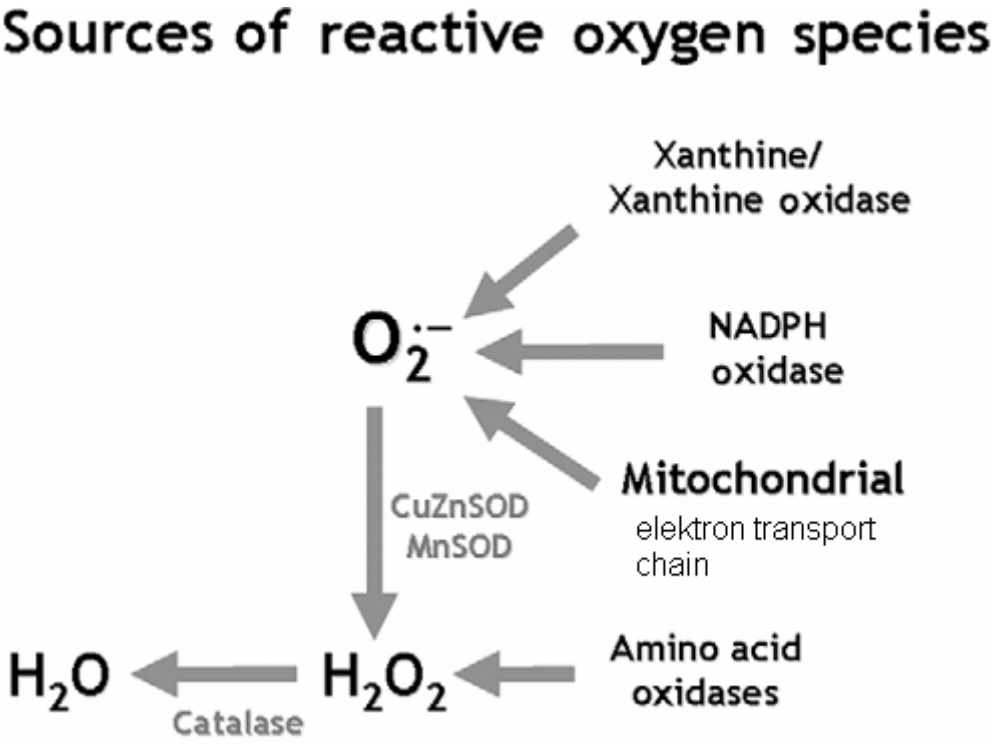

Fig. 1 Cellular and mitochondrial sources of ROS production and breakdown [4]. The mitochondrial electron transport chain, NADPH oxidases, and Xanthine/Xanthine oxidase systems are shown as important sources of $O_2^{=\cdot}$. Superoxide dismutases (CuZn and Mn) convert $O_2^{=\cdot}$ to H_2O_2, which is then broken down to H_2O by catalase and the GSH/glutathione-dependent peroxidase enzyme systems.

4.1.5.2 Negative effects of Reactive oxygen species

When H_2O_2 is produced in excess, it is a toxic molecule which can react with ferrous iron to form $OH^{=}$ [1]. $OH^{=}$ is a short-lived species that can react with DNA [6].

In the mitochondrion, the cooperation of Manganese superoxide dismutase and the GSH/glutathione-dependent peroxidase enzyme system ensures that ROS are kept at a low and nontoxic level. Superoxide dismutases, GSH and GSH/ glutathione-dependent peroxidase systems are part of a powerful defense system in the cell to combat ROS toxicity. But when ROS overcome the

antioxidant defense systems of the cell and redox homeostasis is lost, the result is oxidative stress which can lead to cell damage and death.

It is important to be able to make qualitative and quantitative measurements of ROS production of cells because oxidative stress is part of the pathogenesis and progression of numerous diseases, including neurodegenerative diseases (Huntington, Parkinson, and Alzheimer diseases), retinal degenerative disorders, AIDS, cancer, and the aging process in general.

An interesting research field regarding this case is the identification of proteins which are most susceptible to ROS damage and to use these as potential biomarkers for the early diagnosis of diseases such as Alzheimer diseases [7].

4.2 Interaction between Reactive oxygen species and glutathione

4.2.1 Cell cycle analysis by measurement of Reactive oxygen species

It is common knowledge that intracellular reduction-oxidation environment influences cell cycle progression [8].

For a better understanding of the involved mechanisms Conour JE. et al (2004) used CHO fibroblasts and flow cytometry to measure reduced GSH, ROS, and DNA content with monochlorobimane and 2',7'-dichlorohydrofluorescein diacetate.

GSH content was found to be significantly higher in G2/M compared with G1 phase cells, whereas GSH was intermediate in S phase cells. ROS content stayed at similar levels among all phases. G2/M cells were more reduced than G1 cells. Another conclusion was that GSH- and ROS concentration are related.

So far approaches to define regulatory mechanisms were subjective in nature and focus on single proteins or pathways. To get more information on the issue, the working group mentioned above used protein databases and developed a novel bioinformatic approach to identify possible redox-regulated cell cycle proteins. They concluded that there exists a mechanism that links a variable intracelluar redox environment with cell cycle progression.

4.2.2 Generation of Reactive oxygen species by Cadmium resulting in depletion of glutathione

Cadmium is a non redox-active metal which targets primarily liver cells [9]. J. Liu et al. (2008) found evidence for hydroxyl radical formation in vivo due to Cadmium exposure in hepatocytes of rats. GSH depletion triggered the formation of free radicals. It was stated that the mechanism for Cd-induced oxidative stress is closely correlated with depletion of cellular SH groups and glutathione.

4.2.3 Hyperoxia results in oxidative stress and a response by antioxidant enzymes of the glutathione cycle

Exposure to abnormal high concentrations of oxygen leads to increased generation of ROS [30]. Lushchak et al. (2005) have proven that even in goldfish, an animal which is able to live under high doses of oxygen, activities of glutathione metabolising enzymes are rising under hyperoxia. Despite of its normal behavior a serious oxidative stress was indicated. Activities of glutathione peroxidase and glutathione S-transferase were increased more than catalase and superoxide dismutase during exposure to hyperoxia. Interestingly in some cases glutathione S-transferase was decreased. It is believed that the reason for this event is the fact that glutathione is sensitve for ROS and because of that inactivated.

4.2.4 Depletion of glutathione is necessary for the generation of Reactive oxygen species in Lymphoid cells

GSH depletion is an early sign in apoptosis and GSH efflux during death receptor-mediated apoptosis occurs via a GSH transporter [11].
Franco R. et al (2007) evaluated the relationship between GSH depletion and the generation of ROS in lymphoid cells. At the same time as GSH was depleted, different ROS were generated. Furthermore, depletion of GSH was necessary for generation of ROS, but the other way around, generation of ROS is not necessary for the depletion of GSH.

4.3 Measurement of Cellular state and physiology

4.3.1 Glucose, glutamine and lactate

To gain information about cellular state and physiology a well known practice is to measure glucose and glutamine uptake and lactate production rates with machines consisting of enzyme elektrodes. A common method is to use batch cultures to retrieve sufficient data about state and physiology ranging from maximum cell growth and division till the death of a majority of the cells. In addition viability and concentrations of viable cells are monitored utilising Hemocytometers together with light optical microscopes and Coulter Counter machines. The latter are detecting the change in electrical conductance as a fluid which is containing the cells of interest, is drawn through. Cells, as they are non-conducting particles, alter the effective cross-section of the conductive channel.

4.3.2 Detection of Reactive oxygen species

A widely used compound for the detection of ROS is dichlorofluorescein (DCF). DCF is nonfluorescent until the acetate groups are removed by intracellular esterases and oxidation occurs within the cell.

Esterase cleavage of the lipophilic blocking groups yields a charged form of the dye that is much better retained by cells than is the parent compound.

Oxidation of these probes are detected by monitoring the increase in fluorescence [12]. Schoonen WG. et al. (2005) have chosen dichlorofluorescein diacetate as fluorophore for measurement of ROS formation.

2',7'-Dichlorodihydrofluorescein ($DCFH_2$) is one of the most common used probes for detecting intracellular oxidative stress [9]. It requires a catalyst to be oxidised by hydrogen peroxide or superoxide and reacts nonspecifically with oxidising radicals. Sulfur-centered radicals, also called thiyl radicals, are produced when many radicals are "repaired" by thiols, but are oxidizing agents and through that potentially capable of oxidizing $DCFH_2$.

Rates of oxidation and the yields of DCF were shown to be pH-dependent. GSH-derived radicals interacted with DCF, resulting in the formation of DCFH* absorbing at 390 nm and loss of fluorescence, whereas cysteine-derived radicals did not cause any depletion of DCF fluorescence. Wrona M et al. (2008) stated that the difference in reactivity between glutathione* and Cystein* regarding DCF is related to the formation of carbon-centered, reducing radicals from base-catalyzed isomerization of glutathione*. DCF formation from interaction of $DCFH_2$ with glutathione* was inhibited by oxygen in a concentration-dependent manner within physiological range.

Thus when applying $DCFH_2$ to measure oxidizing radicals in biological systems, we have to consider not only the competition between thiols and $DCFH_2$, but also reactions of thiol-derived radicals plus pH and oxygen concentration, which control the formation of thiyl radicals.

Another application for the detection of ROS is to use it as a tool for medium throughput screening on toxicity [12].

4.3.3 Detection of glutathione

Cell-permeant monochlorobimane which is essentially nonfluorescent until conjugated to thiols, is a thiol-reactive probe for quantitating glutathione levels in cells and for measuring Glutathion S-transferase activity [13].

MCB is reported to react more selectively with glutathione in whole cells than does monobromobimane and has proven useful for assaying drug resistance by flow cytometry.

Already in 1989 MCB was used to label cells aiming at glutathione measurement. COS cells expressing glutathione S-transferase were purified by flow cytometry and used in colony-forming assays to show that glutathione S-transferase delivers cellular resistance to the carcinogen benzo[a]pyrene (+/-)-anti-diol epoxide [14].

Puchalski RB. (1991) used the fact that glutathione S-transferase catalyses the intracellular conjugation of GSH to MCB, and developed a sorting technique to viably seperate recombinant glutathione S-transferase positive cells from the rest, which was electroporated too, but did not express glutathione S-transferase.

Incubation of the hamster cell lines, CHO AB1 and V79, with 10 microM MCB, labeled 75 and 39% of reduced GSH [15]. But incubation of 7 different human cell lines with the same concentration of MCB labeled less than 4% of the total reduced GSH pool. The human cell lines required 1000 microM MCB to label an average of 73% of GSH.

Comparably satisfying results were observed by using 1000 microM MCB to label GSH and flow cytometry on 7 different cell lines (human and rodent), as well as high performance liquid chromatography and standard spectrophotometric analysis. The human and rat glutathione S-transferases

were isolated and purified for steady state kinetic analysis with MCB and GSH as the primary substrates.

Collectively Cook JA. et al. (1991) proofed that MCB fails to label GSH at lower concentrations (less than 50 microM) in human cell lines because of the reduced affinity of MCB for the human transferases. Another possibility would be that there are differences in glutathione S-transferase isozyme expression between rodent and human cell lines.

Raza H. et al. (1991) found that there are existing multiple forms of glutathione S-transferases in rodent and human skin using specific polyclonal antibodies to the Alpha, Mu, and Pi classes of glutathione S-transferases [16].

4.4 Autofluorescence

Background

Autofluorescence is the fluorescence of substances that are part of the cell without addition of any fluophores. It increases the background signal. On one hand this can be problematic in fluorescence microscopy because it can cause structures other than those of interest to become visible. On the other hand, analytical techniques based on auto-fluorescence monitoring can be utilized in order to obtain information about the morphological and physiological state of cells.

Cells contain molecules, which become fluorescent when excited by UV/Vis radiation of specific wavelength [17]. This fluorescence emission by endogenous fluorophores, is an intrinsic property of cells and is called auto-fluorescence to distinguish them from fluorescent signals obtained by adding exogenous markers. The major part of cell auto-fluorescence arises from mitochondria and lysosomes.

The most important endogenous fluorophores are pyridinic acid (NADPH) and flavin coenzymes. Changes occurring in the cell state during physiological and pathological processes result in modifications of the amount of endogenous fluorophores and the chemical-physical properties of their microenvironment.
A decrease in the efficiancy of the metabolism leads to a rising of concentrations of reduced pyridin nucleotids [18]. Level of NADH can be measured through excitation with UV light at 366 nm and detection of emission at 440 nm, while excitation at 436 nm favours emission of flavin at 530 nm. Flavins fluoresce when they are in their oxidised state and fluorescence disappears during reduction [19].

Analytical techniques based on auto-fluorescence monitoring can deliver information about the morphological and physiological state of cells. In addition, auto-fluorescence analysis can be performed in real time because it does not require fixing or staining.

Spectroscopic and imaging techniques have been developed for many different applications in basic research and diagnostics.

5. Aim of the study

The aim of this study was to identify staining protocols that predict cellular stress. These methods could be used for on-line monitoring of cellular physiology during prediction processes.

Two groups of cell lines cultivated in batch processes and analysed: first the CHO host cell lines which were of the dhfr- type and secondly the production cell lines consisting of CHO transfected with EpoFc.

Substrate uptake, lactate production, viable cell count and viability were measured daily. At the same time cellular levels of glutathione (MCB) and ROS (DCFH2) were measured by FACS. In addition, unstained cells were excited at UV and 488 nm wavelengths and their fluorescence signals at 440 and 530 nm respectively were analysed.

6. Material

6.1 Cell lines:

CHO EpoFc 14F2
CHO EpoFc 3F8
CHO EpoFc 1G12
CHO EpoFc 1G7
CHO dhfr-
CHO dhfr- htert 1F12
CHO dhfr- htert 1G4
CHO dhfr- htert neo

6.1.1 CHO EpoFc

CHO EpoFc is a recombinant cell line expressing the fusion protein EpoFc, which comprises two parts, Erythropoetin a peptide linker, and an IgG Fc variant [20].

CHO EpoFc cell lines were cultivated in DMEM HAM´s F12 (1:1)

Supplements:
4 mmol L-Gln
0,25 % sojapeptone
0,1 % pluronic F68
1:100 proteinfree supplement
0,19 mmol MTX

6.1.2 CHO dhfr-

CHO dhfr- (American Type Culture Collection, CRL-9096) is a recombinant cell line which can not express the enzyme dihydrofolate reductase (dhfr). The cell

line is transfected with a vector containing the target gene along with the dhfr marker gene [21]. Selection occurs in the absence of the metabolites hypoxanthine and thymidine and gene amplification is accomplished by exposing the cell line to MTX concentrations, which inhibit dhfr enzyme activity.

Dihydrofolate reductase reduces dihydrofolic acid to tetrahydrofolic acid, using NADPH as electron donor. The product of this reaction is tetrahydrofolate. Inhibition of dhfr can cause folate deficiency and because folate is needed by rapidly dividing cells to synthesize thymidin, this effect may be used as cancer chemotherapy.

CHO dhfr- cell lines were cultivated in DMEM with the following supplements:

Supplements:
4 mmol L-Gln
0,25 % sojapeptone
0,1 % pluronic F68
1:00 proteinfree-supplement
1:100 HT-stocksolution

6.1.3 CHO dhfr- htert

CHO dhfr- htert is transfected with human telomerase (htert). Htert adds hexameric repeats to the chromosome ends and prevents telomeric loss [21]. Over-expression of htert enhances chromosomal stability in CHO cell lines changes the energy metabolism and possibly leads to production stability.

- CHO dhfr- htert neo is transfected with the vector without an insert, functioning as vector controll.

CHO dhfr- htert cell lines were cultivated in DMEM with the following supplements:

Supplements:
4 mmol L-Gln,
0,25 % sojapeptone,
0,1 % pluronic F68,
1:100 proteinfree-supplement,
1:100 HT-stocksolution,
1:250 G418

All cell lines were made available by IAM (Institute for Applied Microbiology), departement for animal cell culture.

All culture media where provided by Biochrome, USA.

6.2 Chemicals:

- Carboxy-2', 7'-dichlorofluorescein

- MCB

- Trypan blue. Trypan blue is an anionic dye from the group of azo colours used for viability staining. Since living cells are very selective in the compounds that pass through their membrane, trypan blue cannot pass and they are not coloured. In dead cells it traverses the membrane and distinctive blue colour is visible under a microscope.

All fluorescence dyes where provided by Molecular Probes.

7. Methods

All cell lines were cultivated in batch process.

7.1 Batch start

- Viability measurement with hemocytometer and trypanblue-labeling.
- Cell count measurement using Coulter Counter machine.
- Calculation of cell suspension- and media-volume.
- Culture media warm up (at 37 °C, Waterbath).
- Transfer calculated amount of media to T-flask.
- Pipette cell suspension into it.
- Transfer to spinner flask.
- Add CO2 (60 ml, injection with sterile filter)
- Incubate at 37 °C on a magnetic stirrer.

7.2 Characterisation of the batch process

Cells were cultivated in spinner flasks on magnetic stirrers at 37 °C
Daily controlling of ph (through observation of the colour of the medium).
Measuring of cell density (cell count), substrate uptake and lactate production at each day.

7.3 Cell count (Coulter Counter)

- Take out 4 ml cellsuspension
- centrifuge
- Supernatant: Allocate 2ml to 2 Eppendorf Tubes, discard the rest.
- Resuspend the pellet in 1 ml triton-citrate-buffer.
- Incubate for 2 hours at room temperature and shake on occasion.
- Measure an appropiate ammount by Coulter Counter, repeat determination.

- Calculation:

  Cellcount [cells/ml] = (result * 9 + cell containing buffervolume) / cell containing buffer volume / 4

  The cell containing buffervolume is depending on the current cell concentration in media.

7.4 Viability (Hemocytometer)

- Attach Coverslip with 70 % Ethanol.
- Move it with gentle pressure untill Newton rings become visible.
- Mix 1 ml fresh cell suspension with 200 µl trypanblue by pipetting up and down in an Eppendorf Tube.
- Fill the counting chambers equally, slowly and free of bubbles.
- Imediately count the cells using a light optical microscope.
- Always count equal numbers of squares per side.
- Count a maximum of 200 cells of living and dead (blue labeled).
- Calculation:

$c = n / V$

c... cell concentration in cells / ml
n... average number of cells / mm^2 area
V... volume counted = 10-4 ml

Every batch lastet untill the viabiliy dropped below 50%.

7.5 Substrate uptake and lactate production

Glucose, lactate and glutamine concentrations of the supernatant were measured by YSI 7100 MBS multiparameter bioanalytical system (YSI Life Sciences, USA)

7.6 Fluorescence measurement

7.6.1 Staining Protocols

7.6.1.1 Reactive Oxygen Species

Carboxy-2',7'-dichlorodihydrofluorescein (H_2DCFDA di(acetoxymethyl ester)

Ex/em FITC like

Stock solution 10 mM in DMSO, 1-10 µM

- 200 µl cell suspension
- 2 µl DAPI
- 2 µl ROS stock (=100 µM)
- incubated 30 minutes at room temperature

7.6.1.2 Glutathione

Monochlorobimane

Ex/em: 350 nm /500 nm

Stock solution 100 mM, Literature 40 µM staining

- 200 µl cell suspension,
- 1 µl stock (=500 µM)
- incubatied for 30 minutes at room temperature

7.6.2 Autofluorescence

Autofluorescence UV: Ex/em: 350 nm/440nm aiming at FAD detection

Autofluorescence 530: Ex/em: 480 nm/530 nm aiming at NADH detection

7.6.3 Fluorescence measurement settings

Only viable cells were analysed using a FACS Vantage (Beckton Dickinson) flow cytometer equipped with Pulse Processing, Sort Enhancement Module and Automatic Cell Deposition Unit.

A 5 W Argon Laser (Coherent), turned to 488 nm, and a 6 W Argon Laser (Spectra Physics), turned to Multi-line-UV, were used. The two lasers are spatially resolved so that no overlap betweeen the respectively excited fluorescence signals can occur. Laser output power was 100 mW for both lines. A 530/30 BP filter was used.

8. Results

8.1 Host cell lines

8.1.1 Viability and cell count

Viability and viable cell concentrations of host cells were satisfyingly similar within repeated batch processes (figure 1). Figure 2C shows that, compared to the other host cells, CHO dhfr- htert 1F12 and CHO dhfr- htert neo showed about twice the viable cell concentrations.

A)

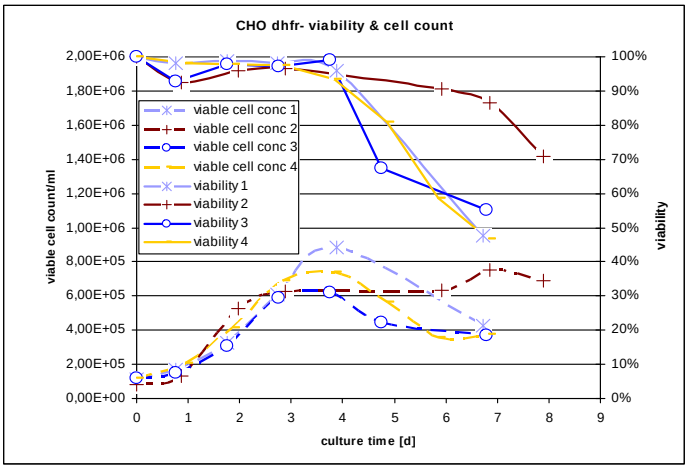

B)

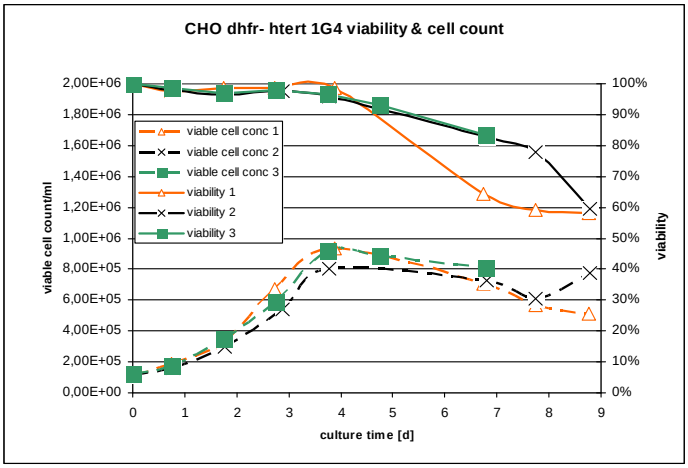

C)

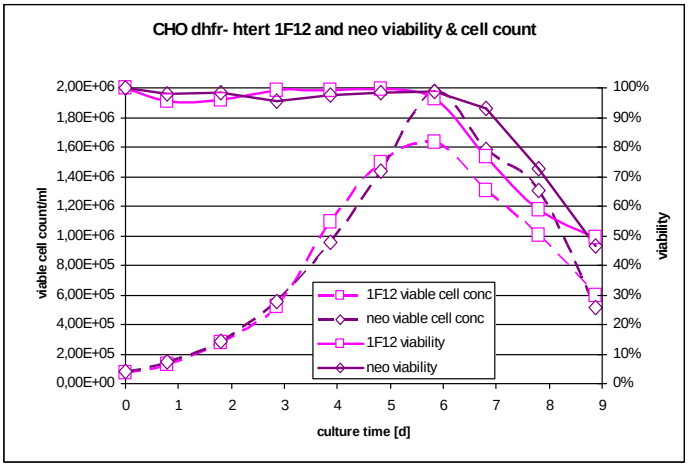

Fig. 2: Viabilities [%] and cell counts [viable cell count/ml]
A: batch 1-4 of CHO dhfr-, B: batch 1-3 of CHO dhfr- htert 1G4, C: CHO dhfr- htert 1F12 and CHO dhfr- htert neo.

8.1.2 Glucose, lactate and glutamine levels

Levels of glucose, lactate and glutamine of all host cell lines were at comparable levels during the whole course of the batch (figures 3-5).

A)

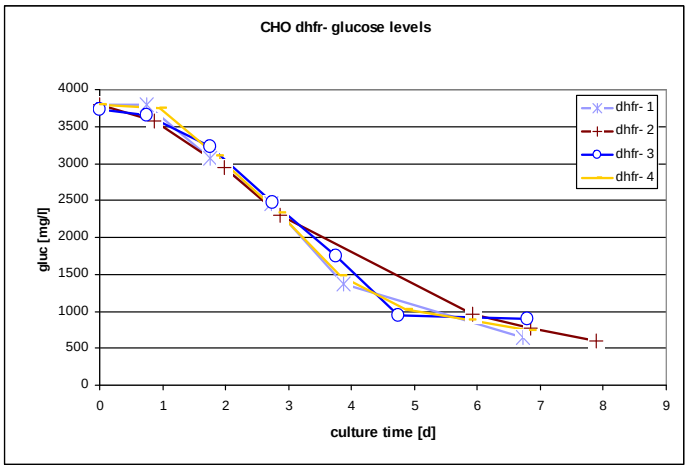

B)

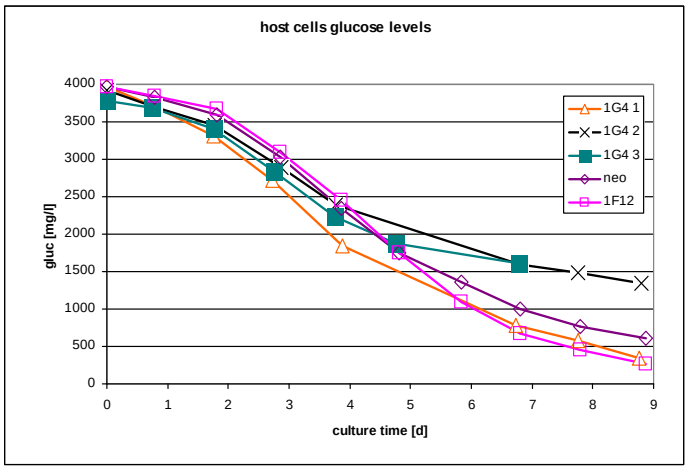

Fig. 3: Glucose levels of all host cell lines [mg/l]

A: batch 1-4 of CHO dhfr-, B: batch 1-3 of CHO dhfr- htert 1G4, C: CHO dhfr- htert 1F12 and CHO dhfr- htert neo.

A)

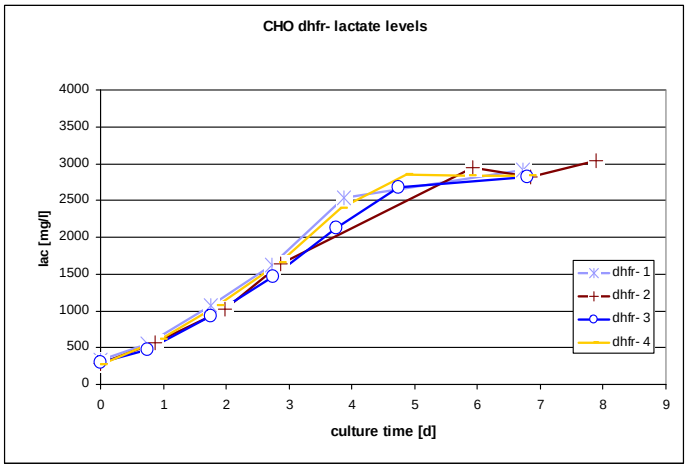

B)

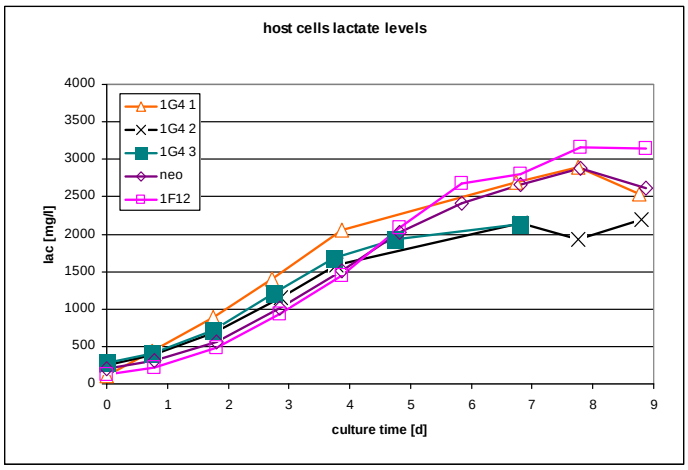

Fig. 4: Lactate levels of all host cell lines [mg/l]

A: batch 1-4 of CHO dhfr-, B: batch 1-3 of CHO dhfr- htert 1G4, C: CHO dhfr- htert 1F12 and CHO dhfr- htert neo.

A)

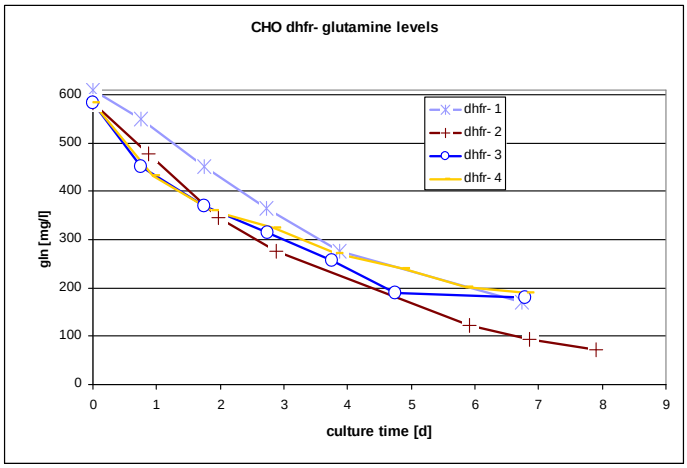

B)

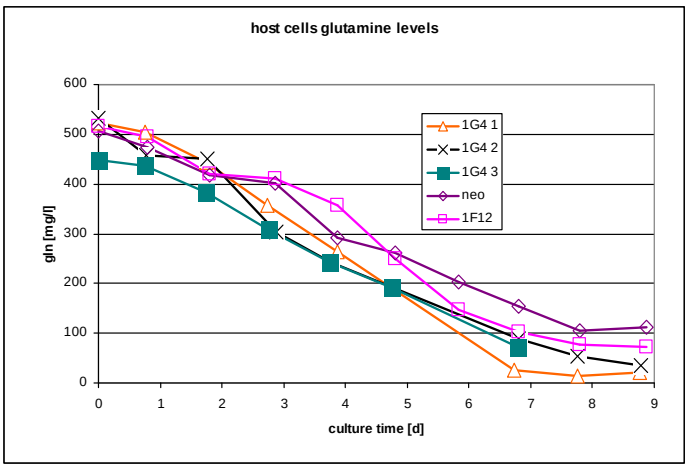

Fig. 5: Glutamine levels of all host cel lines [mg/l]

A: batch 1-4 of CHO dhfr-, B: batch 1-3 of CHO dhfr- htert 1G4, C: CHO dhfr- htert 1F12 and CHO dhfr- htert neo.

Glucose and glutamine uptake and lactate production

The metabolic rates of all host cell lines were at comparable levels during the whole course of the batch (figures 6-8).

A)

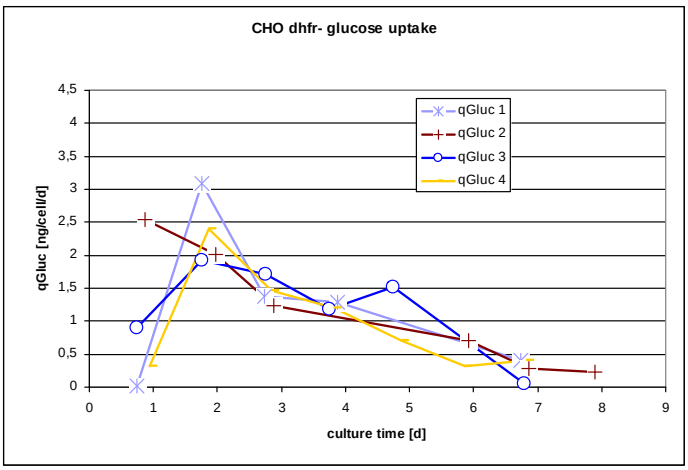

B)

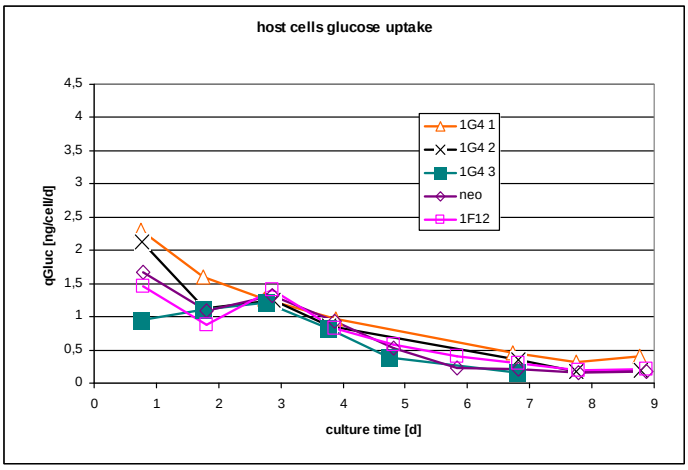

Fig. 6: Cell specific glucose uptake rates of all host cell lines [ng/cell/day]

A: batch 1-4 of CHO dhfr-, B: batch 1-3 of CHO dhfr- htert 1G4, CHO dhfr- 1F12 and CHO dhfr- neo.

A)

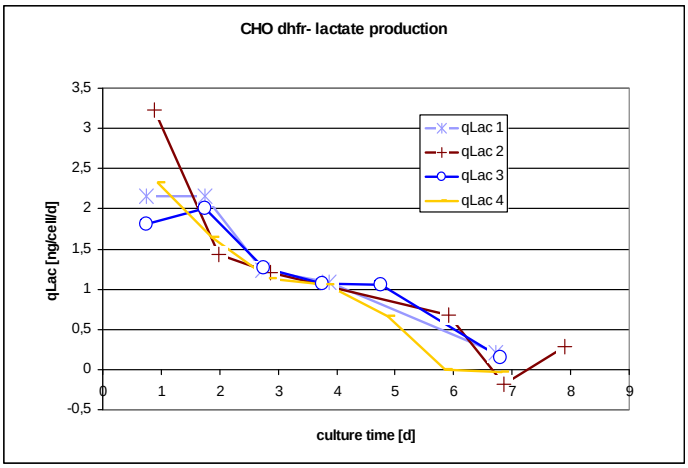

B)

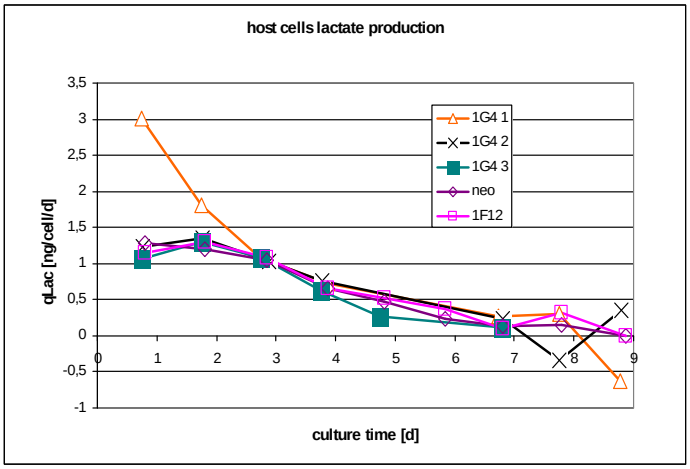

Fig. 7: Cell specific lactate production rates of all host cell lines [ng/cell/day]

A: batch 1-4 of CHO dhfr-, B: batch 1-3 of CHO dhfr- htert 1G4, CHO dhfr- 1F12 and CHO dhfr- neo.

A)

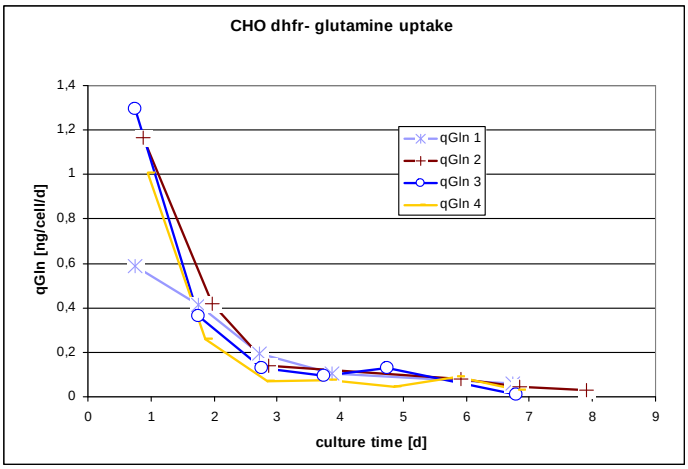

B)

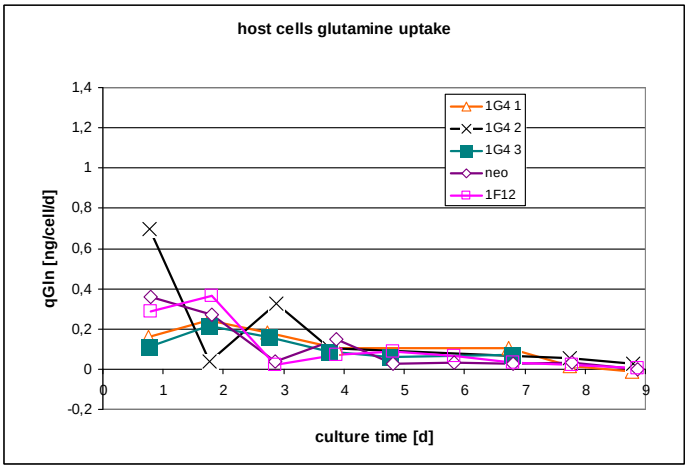

Fig. 8: Cell specific glutamine uptake rates of all host cell lines [ng/cell/day]
A: : batch 1-4 of CHO dhfr-, B: batch 1-3 of CHO dhfr- htert 1G4, CHO dhfr- 1F12 and CHO dhfr- neo.

8.1.3 Fluorescence staining results

Reactive oxygen species

Except for CHO dhfr- batch 3 and CHO dhfr- htert neo (falling ROS levels), levels of ROS were rising towards the end of the batch (figure 9).

A)

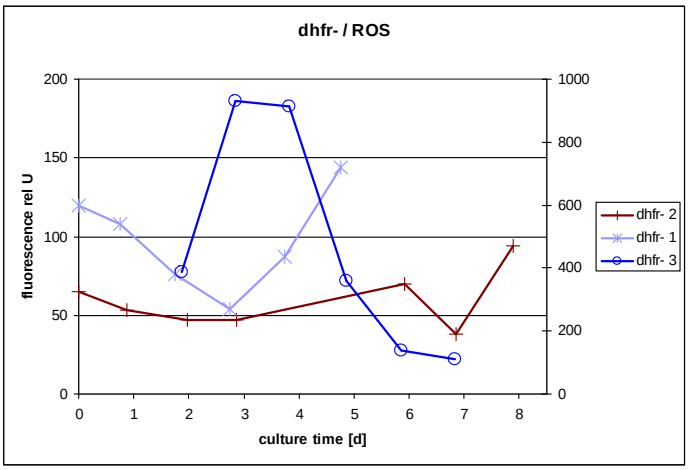

B)

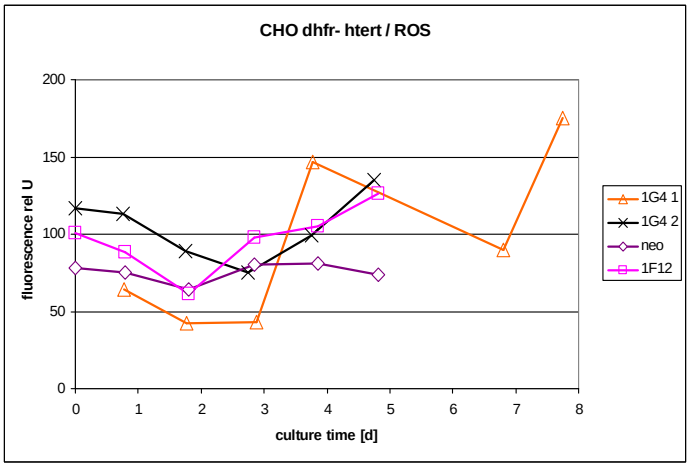

Fig. 9: Levels of intracellular ROS of all host cell lines [relative units]
A: batch 1-3 of CHO dhfr-, B: batch 1-2 of CHO dhfr- htert 1G4, CHO dhfr- 1F12 and CHO dhfr- neo.

Glutathione

Levels of GSH were depleted during the course of every batch process in all analysed host cell lines (figure 10).

A)

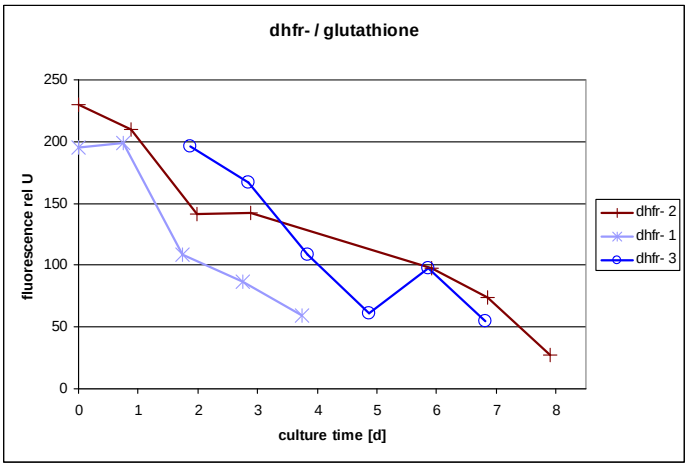

B)

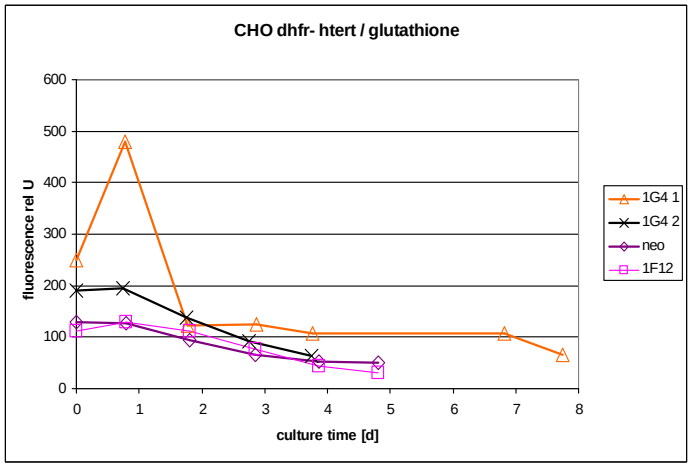

Fig 10: Levels of intracellular glutathione in host cell lines [relative units]
A: batch 1-3 of CHO dhfr-, B: batch 1-2 of CHO dhfr- htert 1G4, CHO dhfr- 1F12 and CHO dhfr- neo.

8.1.4 Autofluorescence

Autofluorescence at UV-light

Levels of autofluorescence excited by UV-light (ex: 350 nm, em: 440 nm) of the host cell lines initially droped and again rised towards the end of all batch cultures (figure 11).

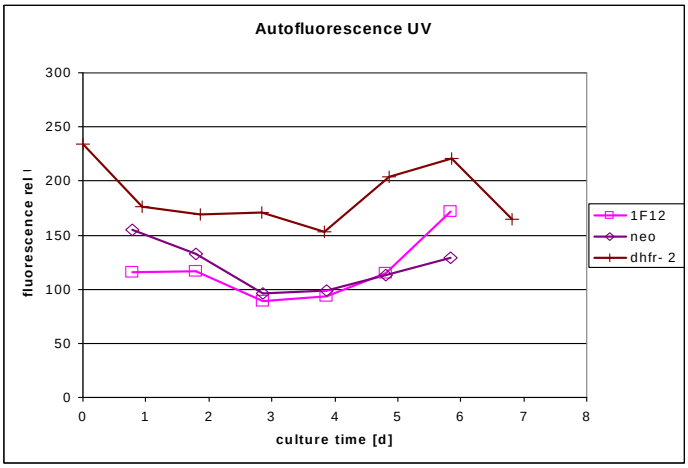

Fig. 11: Autofluorescence levels emitted after excitation with UV light at 350 nm of 3 host cell lines [relative units]

Autofluorescence at green light

Levels of autofluorescence excited by green light (ex: 480 nm, em: 530 nm) of the host cell lines gave a similar pattern of decline and rise as the UV-excited autofluorescence (figure 12).

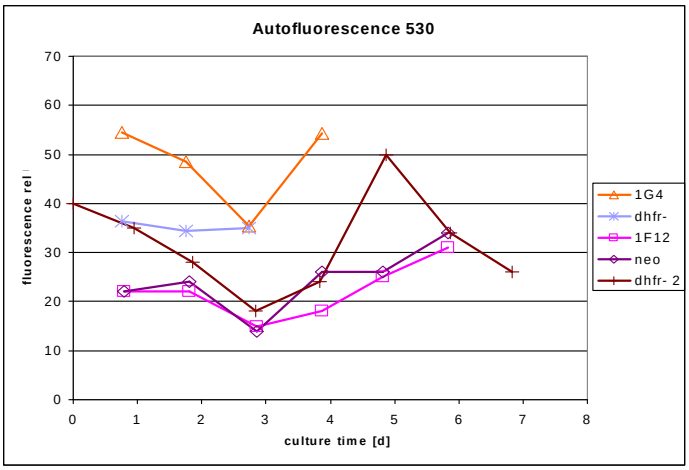

Fig. 12: Autofluorescence levels emitted by host cell lines at 530 nm after excitation of green light at 480 nm [relative units]

8.1.5 Correlations

Correlations between substrate uptake, lactate production and level of Reactive oxygen species

Figures 13 and 14 demonstrate that for all host cells analysed in this study, levels of ROS were low (50 fluorescence relative units) during high substrate concentrations (2500 mg glucose per liter). ROS reached significantly higher levels at day one (between 70 and 110 fluorescence rel units). After substrate depletion, intracellular ROS was rising again. CHO dhfr- batch 3 showed a different pattern from the other two batches.

A)

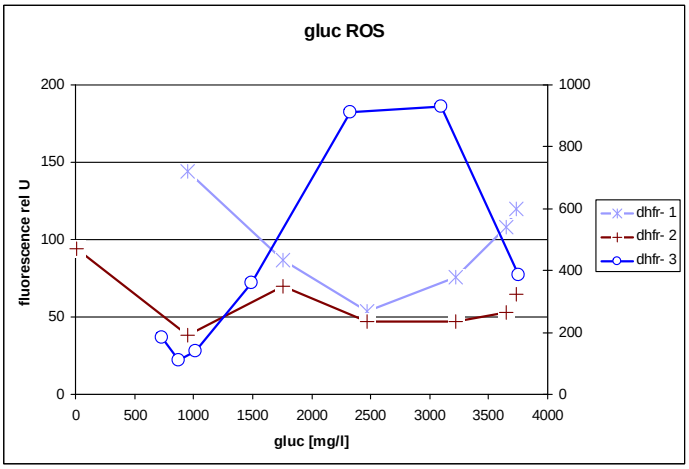

B)

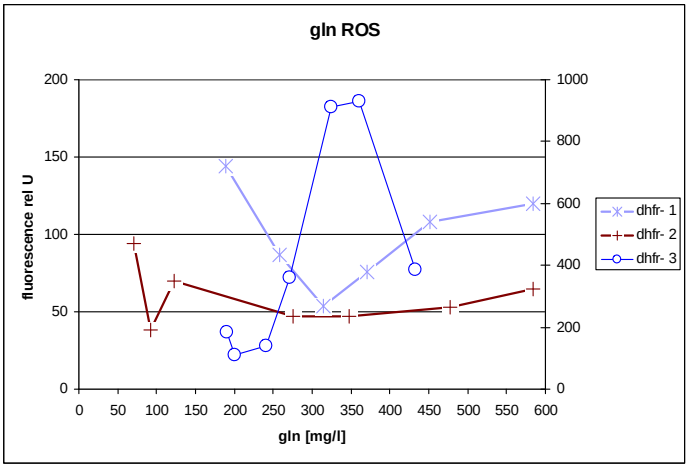

C)

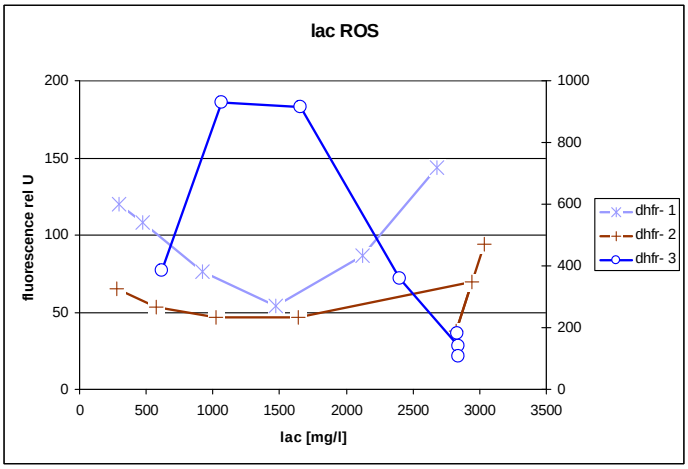

Fig. 13: Correlations between substrate uptake, lactate production and ROS generation of CHO dhfr- cells. A: Glucose uptake against ROS generation, B: Glutamine uptake against ROS production, C: Lactate production against ROS generation

A)

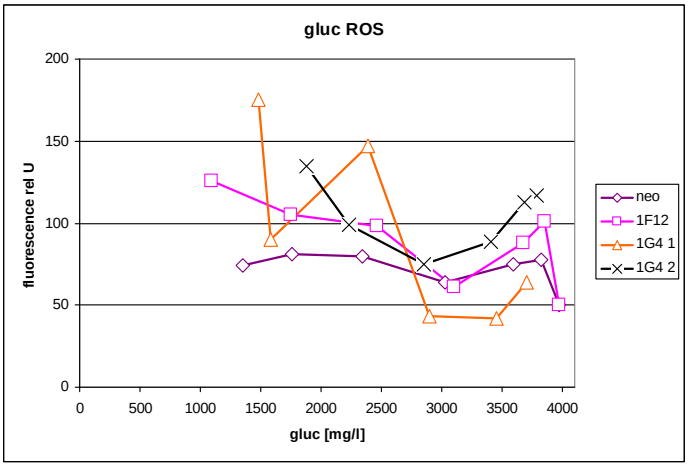

B)

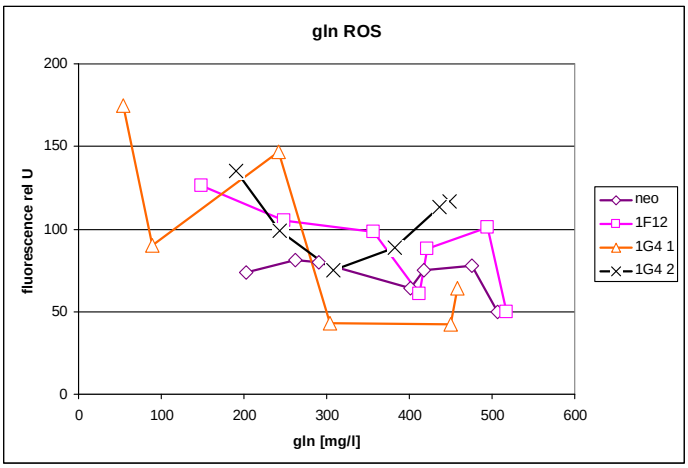

C)

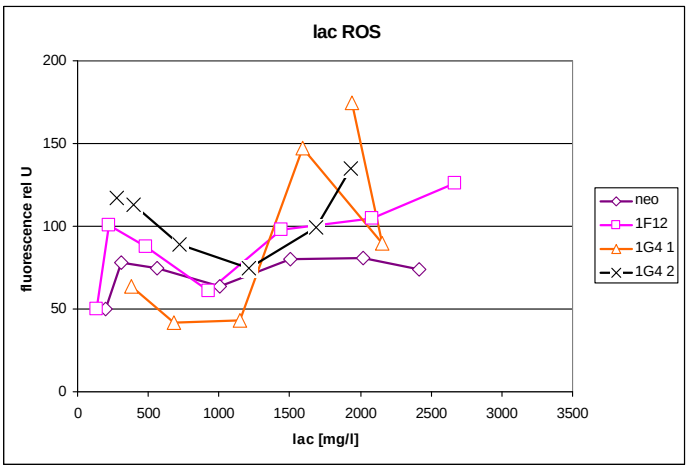

Fig. 14: Correlations between substrate uptake, lactate production and ROS generation of CHO dhfr- htert neo, CHO dhfr- htert 1F12 and CHO dhfr- htert 1G4 batch 1-2

A: CHO dhfr- htert cell lines, ROS against glucose uptake, B: CHO dhfr- htert cell lines ROS against glutamine uptake, C: CHO htert cell lines, ROS against lactate production.

Correlations between metabolic rate and level of Reactive oxygen species

There existed a correlation between glucose uptake rate and ROS levels until maximum of day 4. Figures 13 and 14 show that the best correlation betweeen these two parameters could be measured for CHO dhfr-.

The correlation to lactate production is similar, while for glutamine uptake it is less significant.

A)

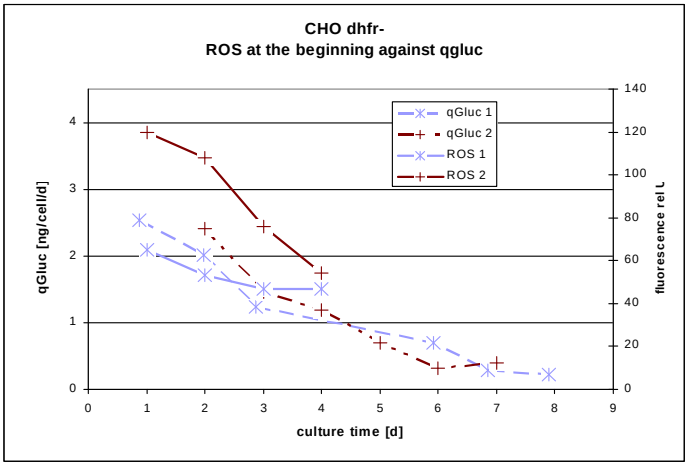

B)

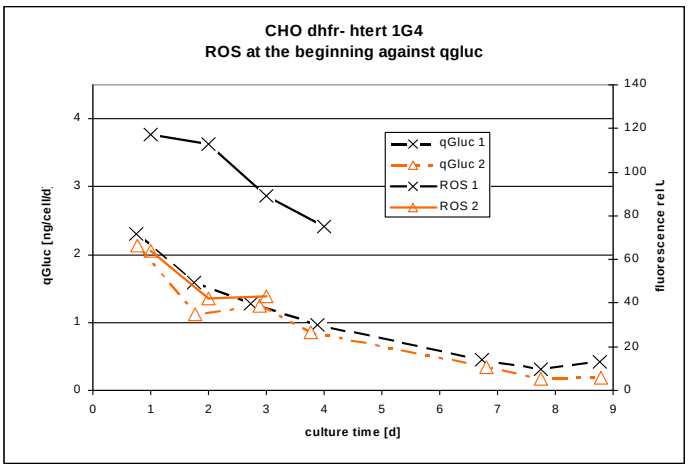

C)

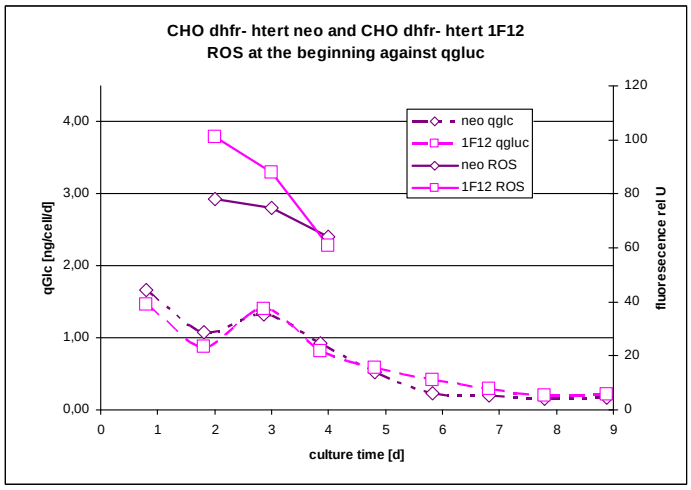

Fig. 15: ROS levels at the beginning of the batch run together with qgluc for all host cell lines A: ROS levels at the day 1-4 of the batch together with qgluc of CHO dhfr-, B: ROS levels at day 1-4 of the batch together with qgluc of CHO htert 1G4, C: ROS levels at day 1-4 of the batch together with qgluc of CHO dhfr- htert neo and CHO dhfr- htert 1F12

A)

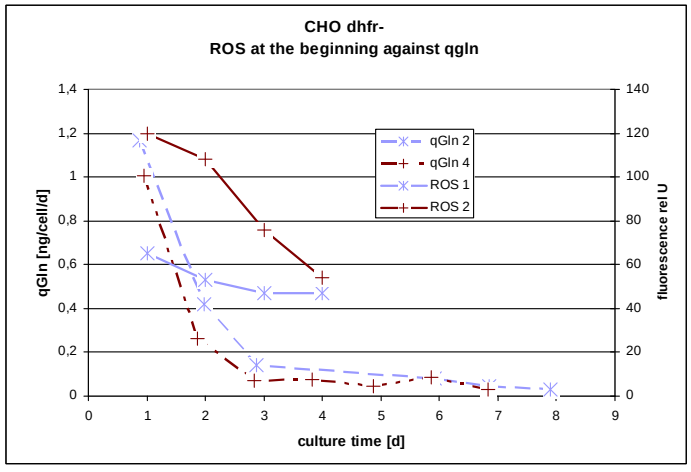

B)

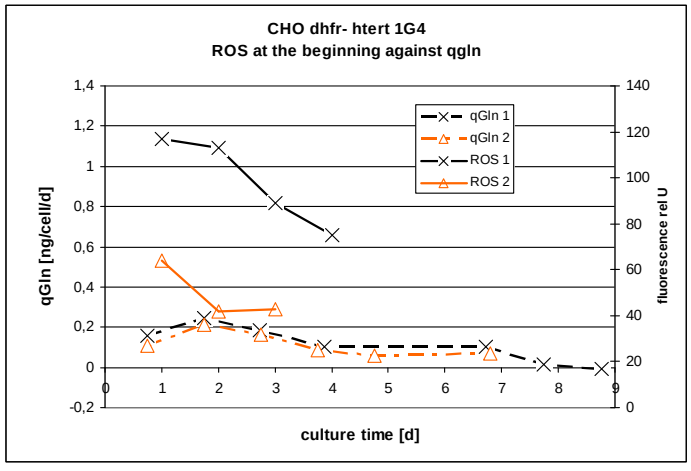

C)

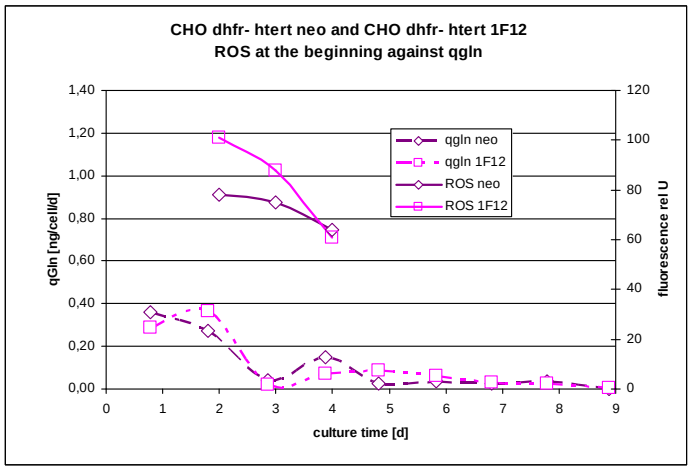

Fig. 16: ROS at he beginning together with qgln for all host cell lines

A: Day 1-4 of ROS levels together with qgln of CHO dhfr-, B: Day 1-4 of ROS together with qgln of CHO dhfr- htert 1G4 batch 1 and day 1-3 of batch 2, C: Day 1-4 of ROS together with qgln of CHO dhfr- neo and CHO dhfr- 1F12.

Correlations between lactate production and level of Reactive oxygen species

There was a correlation between qlac and the levels of ROS at the beginning of every host cell batch (figure 15).

A)

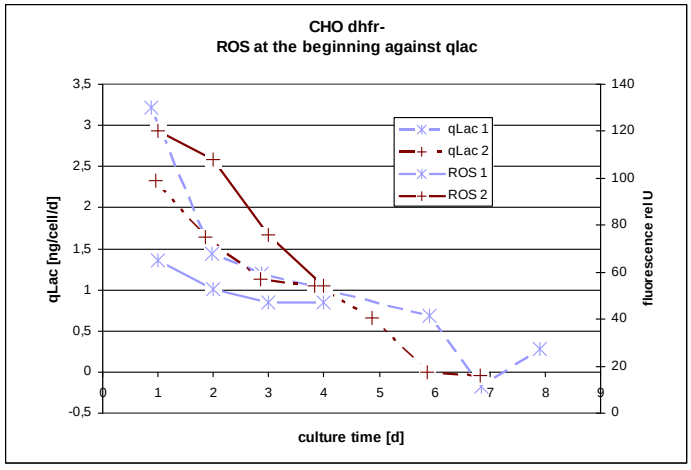

B)

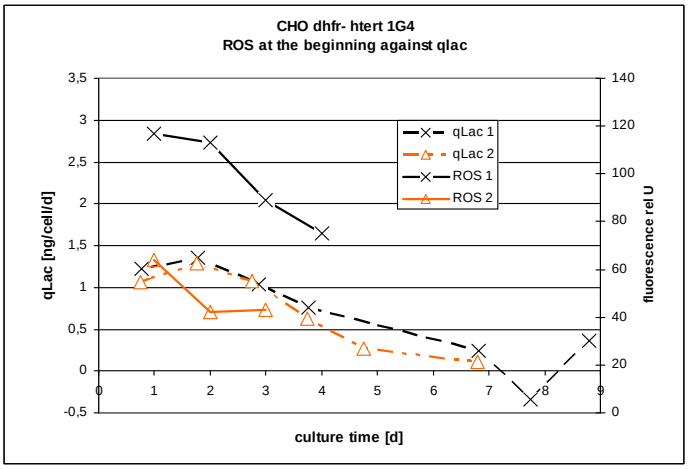

C)

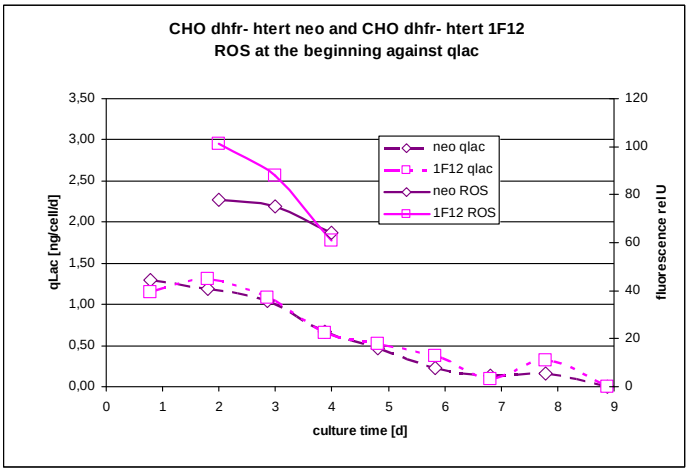

Fig. 17: ROS at he beginning together with qlac for all host cell lines

A: Day 1-4 of ROS levels together with qlac of CHO dhfr-, B: Day 1-4 of ROS levels together with qgluc of CHO htert 1G4 batch 1 (ROS 1) and day 1-3 of batch 2 (ROS 2), C: Day 1-4 of ROS levels together with qlac of CHO dhfr- neo and CHO dhfr- 1F12

Correlations between cellular glutathione and substrate uptake

Cellular glutathione was at constant levels as long as enough substrate was availiable in culture media. Figure 18 and 19 demonstrate that glutathione levels significantly dropped when the glucose concentration was below 1000 mg/l.

A)

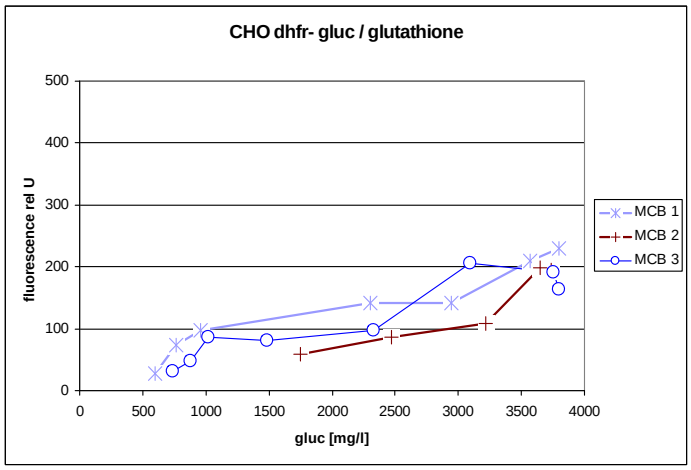

B)

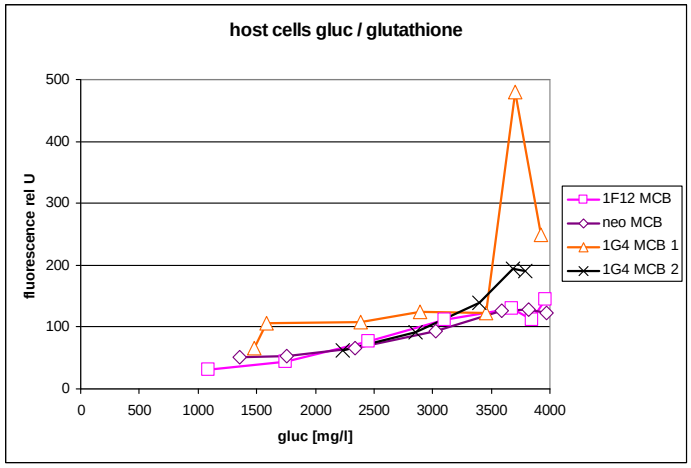

Fig. 18: Glucose uptake levels against glutathione levels of host cell lines

A: Level of glucose uptake against glutathione level of CHO dhfr- batch 1-3 (MCB 1-3), B: Level of glucose uptake against GSH level of the rest of the host cell lines.

A)

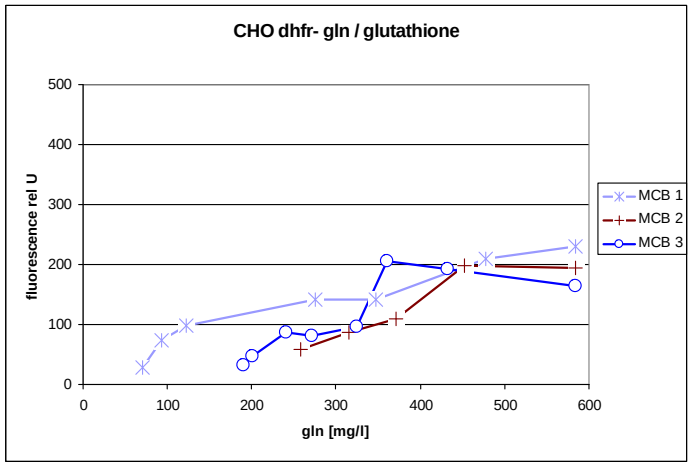

B)

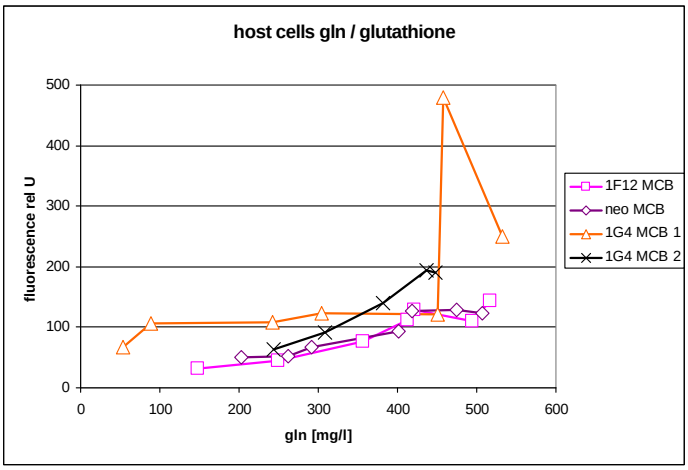

Fig. 19: Glutamine uptake levels against glutathione levels of host cell lines

A: Level of glutamine uptake against glutathione level of CHO dhfr-, B: Level of glutamine uptake against glutathione level of the rest of the host cell lines.

Cellular glutathione and lactate production

There was no correlations between cellular glutathione and lactate production of host cell lines (figure 20).

A)

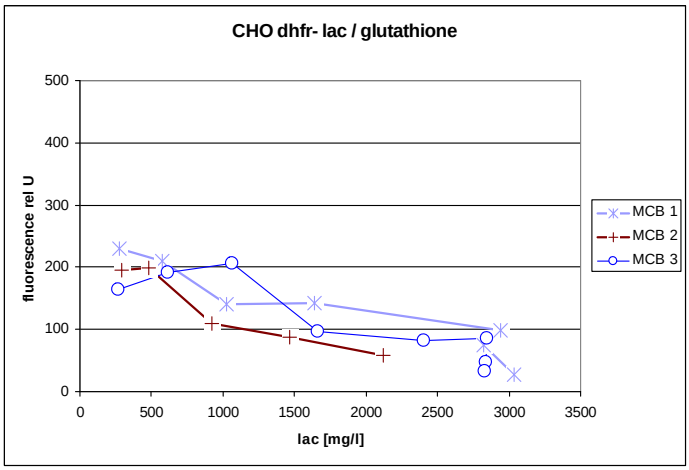

B)

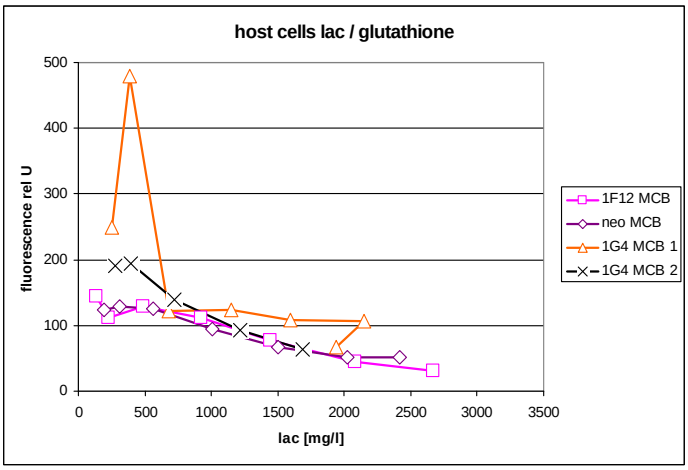

Fig. 20: Lactate production levels against glutathione levels of host cell lines
A: Level of lactate production against GSH level of CHO dhfr-, B: Level of lactate production against GSH level of the rest of the host cell lines.

8.2 Production cell lines

8.2.1 Viability and cell count

Viabilities and viable cell counts of all production cells were at comparable levels when looking at the whole batch experiments (figure 21).

A)

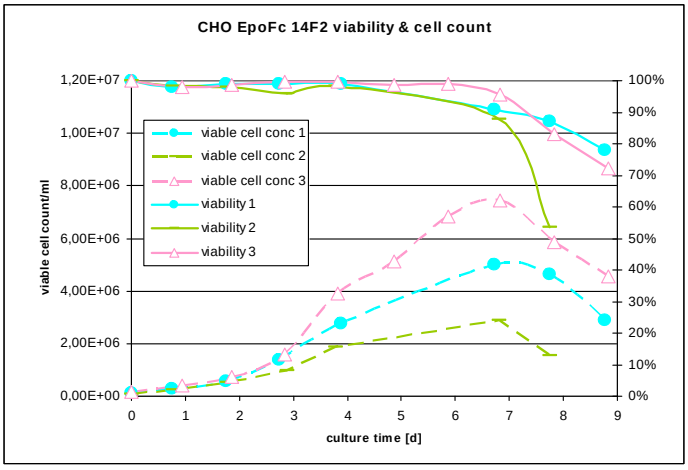

B)

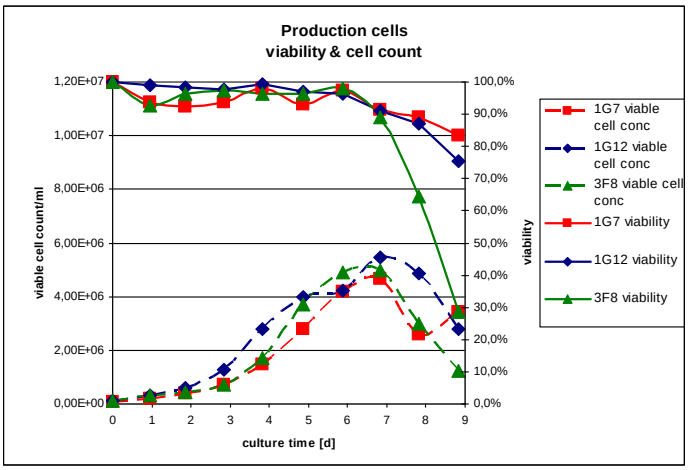

Fig. 21: Viability and cell count of all production cell lines

A: CHO EpoFc 14F2 batch 1-3, B: CHO EpoFc 1G7, CHO epoFc 3F8 and CHO EpoFc 1G12

8.2.2 Glucose, lactate and glutamine levels

Glutamine and glucose were depleted and lactate was rising during every production cell batch.

A)

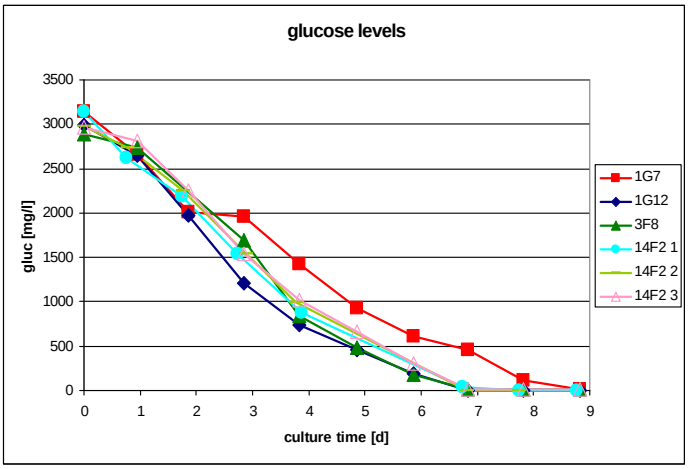

B)

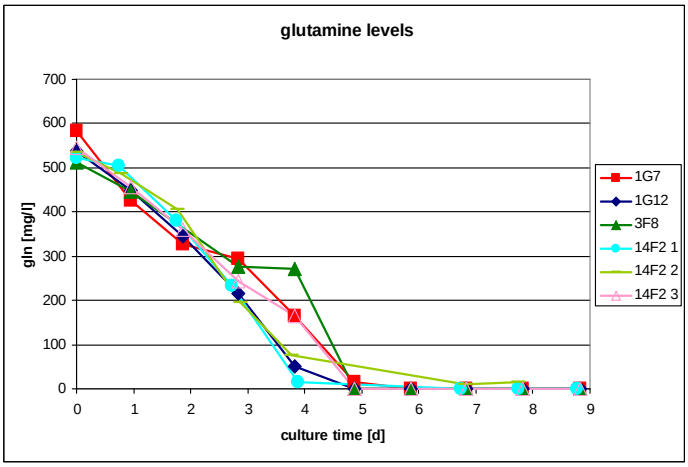

C)

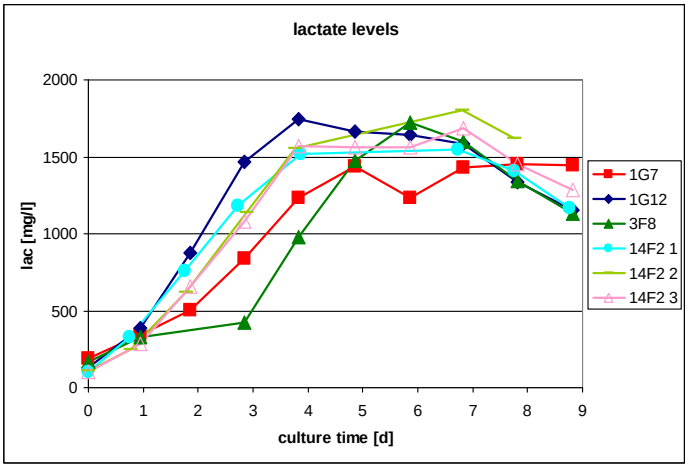

Fig. 22: Glucose, glutamine and lactate levels of all production cell lines [mg/l]
A: Glucose levels, B: Glutamine levels, C: Lactate levels

Metabolic rates fell from about 3 to nearly 0 ng per cell per day in 4 days. Glutamine was taken up almost completely in the same time (figure 23 A and B). Lactate production was reduced in a way typical for all observed batch processes during this study (figure 23 C).

A)

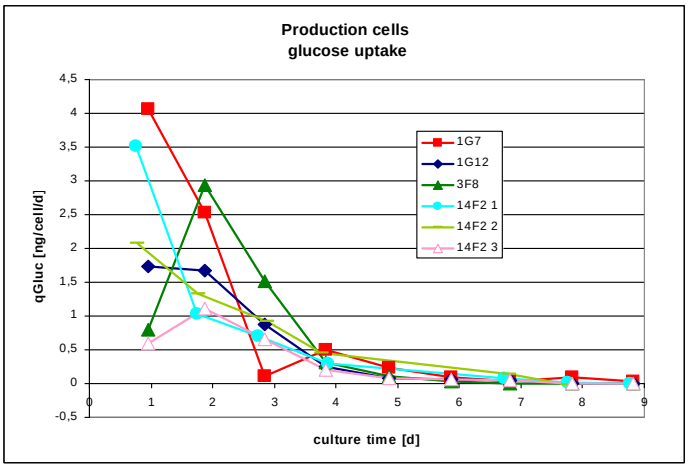

B)

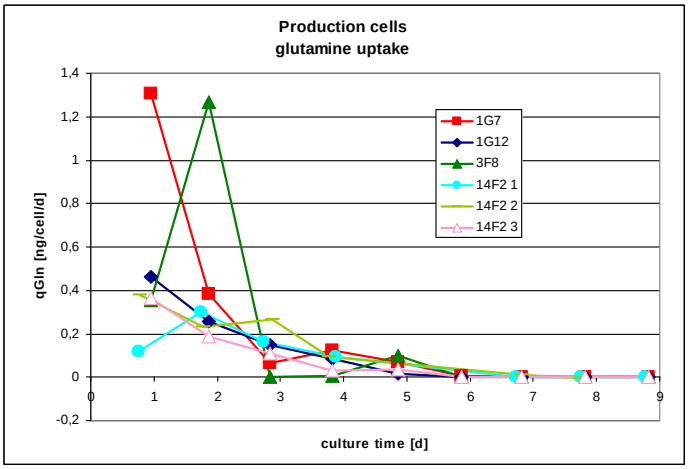

C)

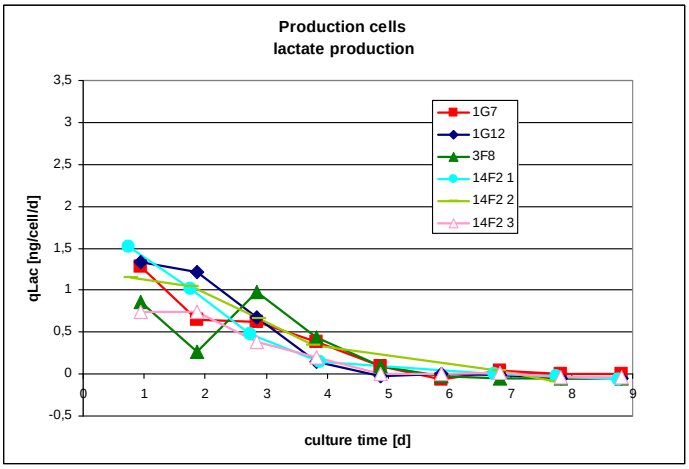

Fig. 23: Glucose uptake, glutamine uptake and lactate production [ng/cell/day]

A: Glucose uptake, B: Glutamine uptake, C: Lactate production

8.2.3 Fluorescence staining results

Reactive oxygen species levels

ROS levels were rising until the maxium of day 3 and depleting till the end. The only exception was batch 1 of CHO EpoFc 14F2 (figure 24).

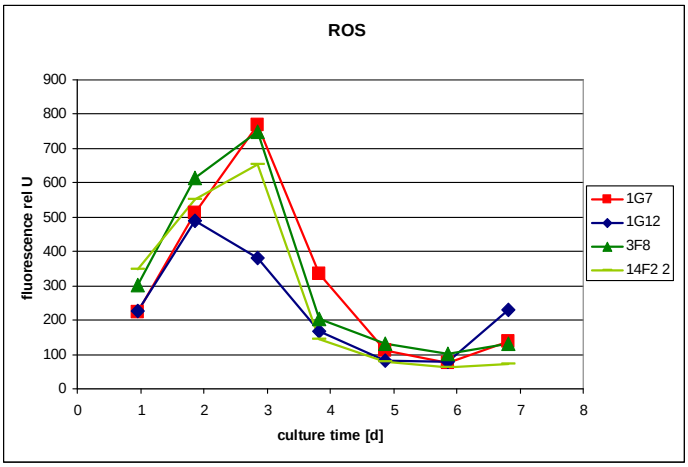

Fig. 24: Levels of Reactive oxygen species for 4 production cell lines [relative units]
1G7: CHO EpoFc 1G7, 1G12: CHO EpoFc 1G12, 3F8: CHO EpoFc 3F8, 14F2 2: CHO EpoFc 14F2 batch 2

Glutathione levels

GSH contantly declined from the start to the end of every analysed production cell line batch (figure 25).

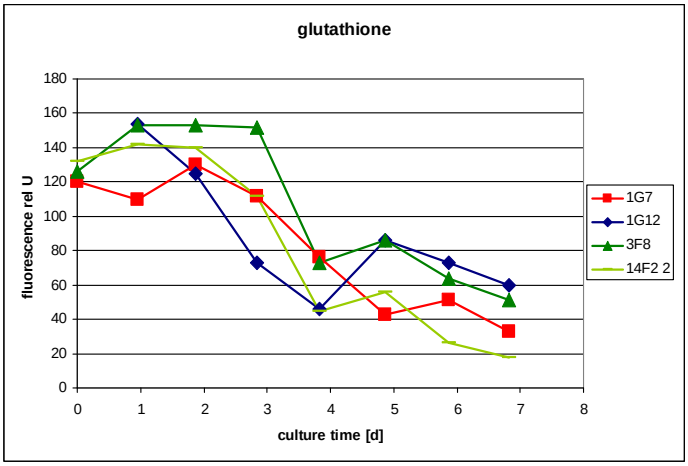

Fig. 25: Levels of glutahione for 4 production cell lines [relative units]
1G7: CHO EpoFc 1G7, 1G12: CHO EpoFc 1G12, 3F8: CHO EpoFc 3F8, 14F2 2: CHO EpoFc 14F2 batch 2

8.2.4 Autofluorescence

Levels of Autofluorescence at UV-light

Levels of autofluorescence at UV-light were characterised by signific peaks on day 2 and 5 of every culture (figure 26).

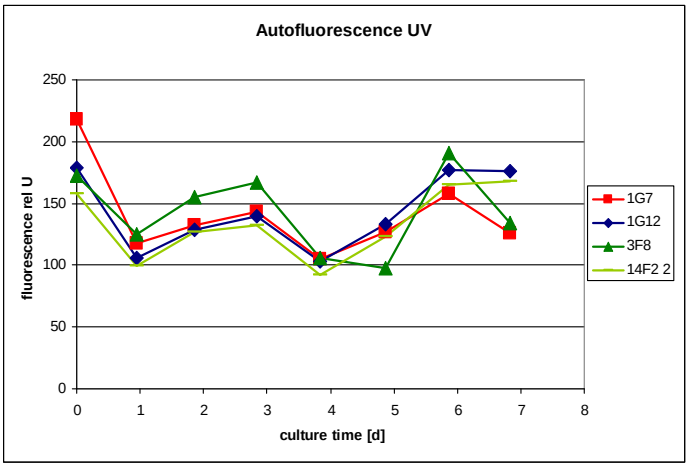

Fig. 26: Levels of autofluorescence excited by UV light for 4 production cell lines [relative units]
1G7: CHO EpoFc 1G7, 1G12: CHO EpoFc 1G12, 3F8: CHO EpoFc 3F8, 14F2 2: CHO EpoFc 14F2 batch 2

Levels of Autofluorescence at 530 nm

Levels of autofluorescence at 530 nm showed one peak at day 1, a minimum on day 3 and were rising till the end (figure 27). Only exception was batch 1 of CHO EpoFc 14F2, which was constantly rising.

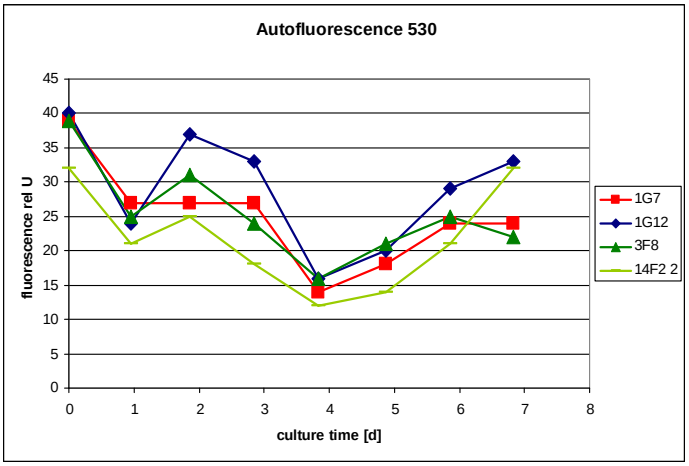

Fig. 27: Levels of autofluorescence at 530 nm for 4 production cell lines [relative units]
1G7: CHO EpoFc 1G7, 1G12: CHO EpoFc 1G12, 3F8: CHO EpoFc 3F8, 14F2 2: CHO EpoFc 14F2 batch 2

8.2.5 Correlations

Reactive oxygen species substrate uptake and lactate production

In all production cell lines levels of ROS reached their highest numbers when amount of substrate was half depleted (1500 mg glucose and 300 mg glutamine, figure 28A and B).

Right after this peak ROS levels fell down to minium levels. Lactate production underlines this behaviour as the ROS levels were the opposite of the ones measured for the substrate uptake (figure 28C).

A)

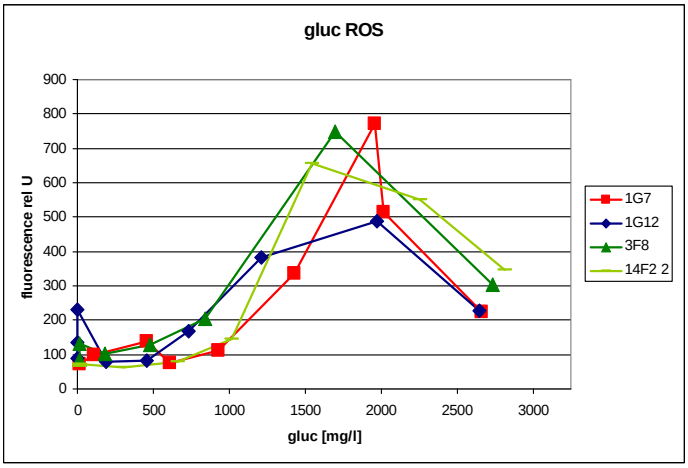

B)

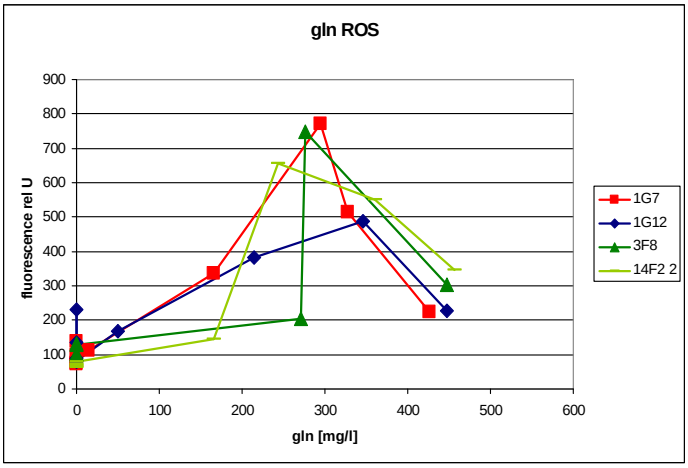

C)

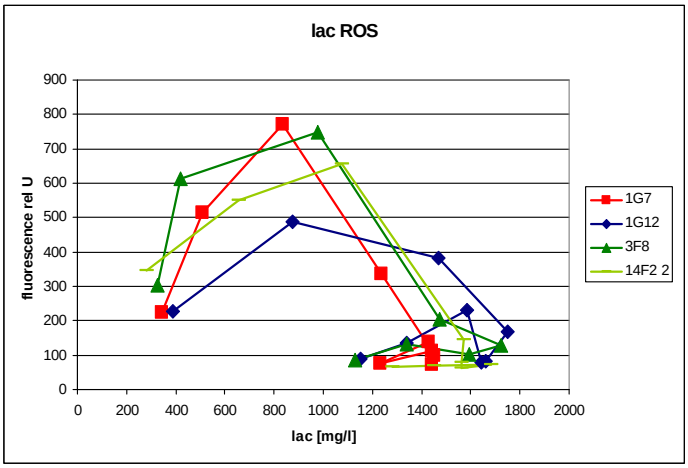

Fig. 29: Substrate uptake and lactate production against ROS levels of 4 production cell lines. A: Glucose uptake against ROS levels, B: Glutamine uptake against ROS levels, C: lactate production against ROS levels

1G7: CHO EpoFc 1G7, 1G12: CHO EpoFc 1G12, 3F8: CHO EpoFc 3F8, 14F2 2: CHO EpoFc 14F2 batch 2

Correlations between energy uptake rate and level of Reactive oxygen species

There were no correlations between ROS concentration and energy uptake rate observed for all production cell lines (figure 30).

A)

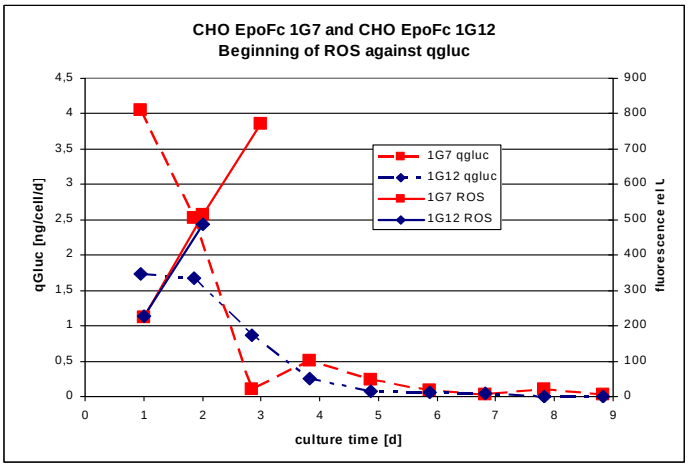

B)

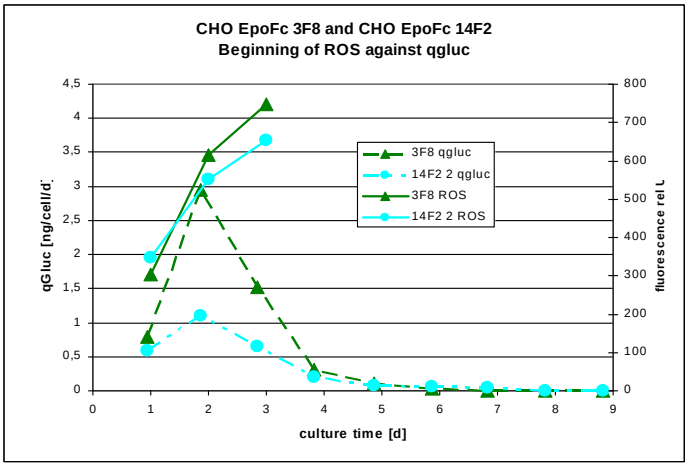

Fig. 30: First days of ROS together with qgluc

A: First three days of ROS levels against qgluc of CHO EpoFc 1G7 and CHO EpoFc 1G12, B: First three days of ROS levels against qgluc of CHO EpoFc 3F8 and CHO EpoFc 14F2 batch 2

Correlations between cellular glutathione, substrate uptake and lactate production

Level of cellular GSH declined with the amount of availiable glucose and glutamine during all analysed batch processes. Figure 31 is showing that the less substrate is present in culture media, the lower were the detected levels of GSH.

A)

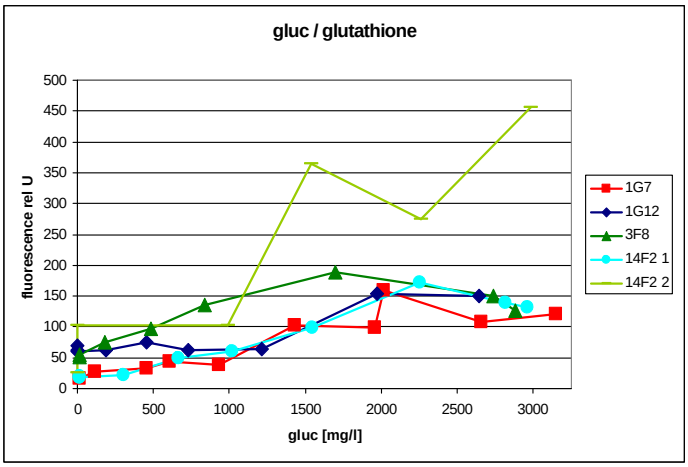

B)

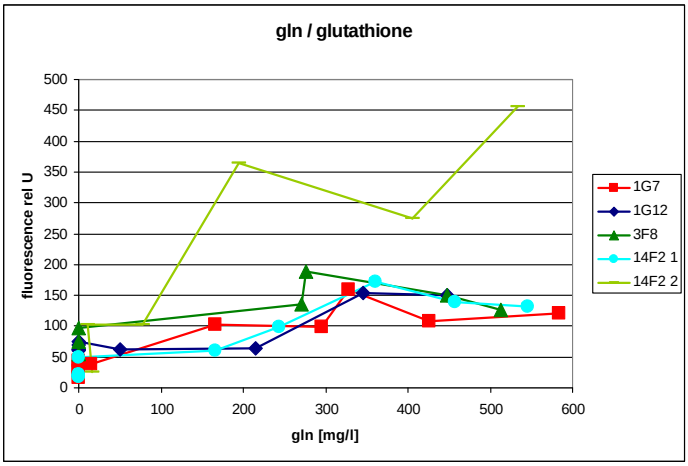

C)

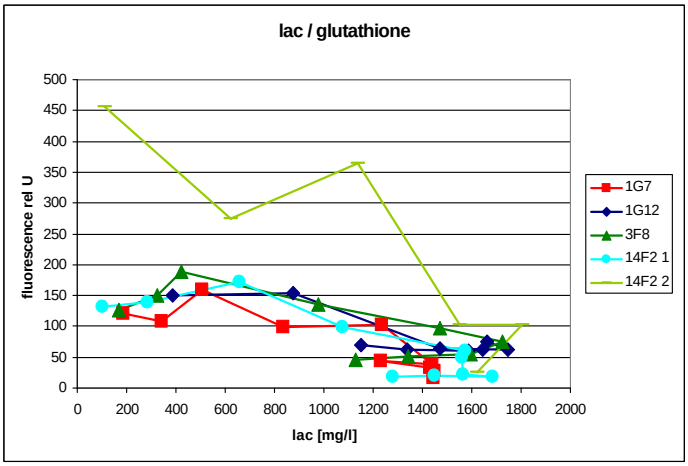

Fig. 31: Substrate uptake and lactate production against glutathione levels of all production cell lines

A: Glucose levels against GSH levels, B: Glutamine levels against GSH levels, C: Lactate levels against glutathione levels

9. Discussion

As mentioned at the beginning of this work, ROS are accumulating in cells when they suffer from different forms of stress. An important source of ROS is the mitochondrial metabolism [4]. Other causes can be photooxidation end emissions [7].

The measured levels of ROS in the host cells fitted to the prognosted behaviour (figure 9), but in production cells the ROS level were high when cells where in good condition due to high substrate quantities and fell off following viability and viable cell concentration towards the end of every batch (figure 24).
An explanation for the different symptoms could be that glutathione disulfide is needed for GSH regeneration and in production cells glutathione disulfide is much more needed in the endoplasmatic reticulum to form disulfide bonds of the produced proteins than in host cells.

An interesting thing to see was that the energy uptake rate of host cells correlated to levels of ROS until day 4 (figures 15-17). In production cell lines there was no such correlation measured at all (figure 30).

Levels of glutathione were significantly higher during the first half than at the end of all batch experiments (figures 10 and 25). This fits to the fact that in the cell GSH is a part of the defense system against ROS, and the maintainance of intracellular GSH levels is very energy dependent [1]. As substrate is depleted the cellular defense breaks down. The conclusion would be that ROS levels were increasing at the last days of all batches, but as described above this was only true for host cells.

Levels of autofluorescence at both wavelengths (440 nm and 530 nm) initially droped and rised again towards the end of all analysed batch cultures.
Detected autofluorescence was high when cellular state was bad (figures 11, 12, 26 and 27). It is believed that autofluorescence is correlated to diseases which are often started by metabolic stress [22]. The observed results fit into this thesis as stress is significantly higher at the end of every batch.

Especially ROS and GSH measurment in combination give a good indication of the present stress level in the culture.

10. References

1. Halliwell, B., and Gutteridge, J. M. (1999). ‘‘Free Radicals in Biology and Medicine.’’ Oxford University Press, UK

2. Shenker BJ, Mayro JS, Rooney C, Vitale L, Shapiro IM (1993) Immunotoxic effects of mercuric compounds on human lymphocytes and monocytes. IV. Alterations in cellular glutathione content. Immunopharmacol Immunotoxicol. Mar-Jun;15(2-3):273-90.

3. Xu L, Koumenis IL, Tilly JL, Giffard RG (1999) Overexpression of bcl-xL protects astrocytes from glucose deprivation and is associated with higher glutathione, ferritin, and iron levels. Anesthesiology. Oct;91(4):1036-46

4. Lambert, A. J., and Brand, M. D. (2004). Inhibitors of the quinone-binding site allow rapid superoxide production from mitochondrial NADH: Ubiquinone oxidoreductase (complex I). J. Biol. Chem. 279, 39414–39420.

5. Li, Y., Huang, T. T., Carlson, E. J., Melov, S., Ursell, P. C., Olson, J. L., Noble, L. J., Yoshimura, M. P., Berger, C., Chan, P. H., Wallace, D. C., and Epstein, C. J. (1995). Dilated cardiomyopathy and neonatal lethality in mutant mice lacking manganese superoxide dismutase. Nat. Genet. 11, 376–381

6. J. S. Armstrong and M. Whiteman, Department of Biochemistry, Yong Loo Lin (2007) Measurement of Reactive Oxygen Species in Cells and Mitochondria METHODS IN CELL BIOLOGY, VOL. 80, Chapter 18.

7. Gracy RW, Talent JM, Kong Y, Conrad CC (1999) Reactive oxygen species: The unavoidable environmental insult? Mutation research Jul 16;428(1-2):17-22

8. Conour JE, Graham WV, Gaskins HR (2004) A combined in vitro/bioinformatic investigation of redox regulatory mechanisms governing cell cycle progression. Physiol Genomics. Jul 8;18(2):196-205.

9. Jie Liu, Steven Y. Quian, Qiong Guo, JinJie Jiang, Michael P. Waalkes, Ronald P. Mason, Maria B. Kadiiska (2008) Cadmium generates reactive oxygen- and carbon-centered radical species in rats . Insights from in vivo spin-trapping studies. Free Radiacal Biology & Medicine 45, 475-481

10. Volodymyr I. Lushchak, Tetyana V. Bagnyukova, Victor V. Husak, Lidiya I. Luzhna, Oleh V. Lushchak, Kenneth B. Storey (2005). Hyperoxia results in transient oxidative stress and an adaptive response by antioxidant enzymes in goldfish tissues. The International Journal of Biochemistry & Cell Biology 37. 1670-1080

11. Franco R, Panayiotidis MI, Cidlowski JA (2007) Glutathione depletion is necessary for apoptosis in lymphoid cells independent of reactive oxygen species formation. J Biol Chem. Oct 19;282(42):30452-65.

12. Schoonen WG, Westerink WM, de Roos JA, Débiton E (2005) Cytotoxic effects of 100 reference compounds on Hep G2 and HeLa cells and of 60 compounds on ECC-1 and CHO cells. I mechanistic assays on ROS, glutathione depletion and calcein uptake. Toxicol In Vitro. Jun;19(4):505-16

13. Cook JA, Pass HI, Russo A, Iype S, Mitchell JB (1989) Use of monochlorobimane for glutathione measurements in hamster and human tumor cell lines. Int. J. Radiat. Oncol. Biol. Phys. May; 16(5): 132 1-4.

14. Puchalski RB, Manoharan TH, Lathrop AL, Fahl WE (1991) Recombinant glutathione S-transferase (GST) expressing cells purified by flow cytometry on the basis of a GST-catalyzed intracellular conjugation of glutathione to monochlorobimane. Cytometry.12(7):651-65.

15. Cook JA, Iype SN, Mitchell JB (1991) Differential specificity of monochlorobimane for isozymes of human and rodent glutathione S-transferases. Cancer Res. Mar 15;51(6):1606-12.

16. Raza H, Awasthi YC, Zaim MT, Eckert RL, Mukhtar H (1991) Glutathione S-transferases in human and rodent skin: multiple forms and species-specific expression. J Invest Dermatol. Apr;96(4):463-7.

17. Monici M (2005) Cell and tissue autofluorescence research and diagnostic applications. Biotechnol Annu Rev.;11:227-56.

18. A. C. Croce', A. Spano', D. Locatelli', S. Barnil, L. Sciola, G. Bottiroli (1999) Dependence of Fibroblast Autofluorescence on Normal and Transformed Conditions. Role of the Metabolic Activity. Photochemistry and Photobiology 69(3): 364-374

19. Bo Thorell (1983) Flow-Cytometric Monitoring of Intracellular Flavins Simultaneously With NAD(P)H Levels. Cytometry 4: 61-65

20. .Kornelia Schriebl, Evelyn Trummer, Christine Lattenmayer, Robert Weik, Renate Kunert, Dethardt Müller, Hermann Katinger, Karola Vorauer-Uhl (2006) Biochemical characterization of rhEpo-Fc fusion protein expressed in CHO cells. Protein Expression and Purification 49. October, Pages 265-275

21. Darrin Kuystermans, Britta Krampe, Halina Swiderek, Mohamed Al-Rubeai (2007) Using cell engineering and omic tools for the improvement of cell culture processes Cytotechnology 53: 3–22

22. Elner VM, Park S, Cornblath W, Hackel R, Petty HR (2008) . Flavoprotein autofluorescence detection of early ocular dysfunction. Arch Ophthalmol Feb;126(2):259-60.